HHS Public Access

Author manuscript

*J Control Release*. Author manuscript; available in PMC 2024 July 01.

Published in final edited form as:

*J Control Release*. 2024 January ; 365: 848–875. doi:10.1016/j.jconrel.2023.09.025.

# Natural medicine delivery from 3D printed bone substitutes

**Susmita Bose**[*], **Naboneeta Sarkar**[1], **Yongdeok Jo**[1]

W. M. Keck Biomedical Materials Research Laboratory, School of Mechanical and Materials Engineering, Washington State University, Pullman, WA 99164, United States

## Abstract

Unmet medical needs in treating critical-size bone defects have led to the development of numerous innovative bone tissue engineering implants. Although additive manufacturing allows flexible patient-specific treatments by modifying topological properties with various materials, the development of ideal bone implants that aid new tissue regeneration and reduce post-implantation bone disorders has been limited. Natural biomolecules are gaining the attention of the health industry due to their excellent safety profiles, providing equivalent or superior performances when compared to more expensive growth factors and synthetic drugs. Supplementing additive manufacturing with natural biomolecules enables the design of novel multifunctional bone implants that provide controlled biochemical delivery for bone tissue engineering applications. Controlled release of naturally derived biomolecules from a three-dimensional (3D) printed implant may improve implant-host tissue integration, new bone formation, bone healing, and blood vessel growth. The present review introduces us to the current progress and limitations of 3D printed bone implants with drug delivery capabilities, followed by an in-depth discussion on cutting-edge technologies for incorporating natural medicinal compounds embedded within the 3D printed scaffolds or on implant surfaces, highlighting their applications in several pre- and post-implantation bone-related disorders.

### Keywords

3D printing; Bone implant; Drug delivery; Natural products; Herbal medicine

## 1. Introduction

The human body is supported by the skeletal system, which consists of bones, cartilage, ligaments, and tendons. The skeleton protects the internal organs and stores vital minerals, while bone marrow produces blood [1]. Bone tissue can remodel itself through a close interplay between bone-resorbing osteoclast cells that digest old or damaged bone and bone-forming osteoblast cells that deposit new bone material. Every year, worldwide incidences of

[*] Corresponding author. sbose@wsu.edu (S. Bose).

[1] Equal contribution.

Declaration of Competing Interest

The authors declare no conflicts of interest. This content is solely the authors' responsibility and does not necessarily represent the official views of the National Institutes of Health.

bone diseases and other bone-related complications, including bone infection, bone tumor, and bone loss, have increased due to growing life expectancy and the aging population [2,3]. Natural bone undergoes constant remodeling; however, it is unable to heal large bone defects by itself, also known as critical-sized bone defects. These are generally caused by severe infection, osseous abnormalities, trauma, and tumor resection [4]. To treat such defects, surgical procedures are stringently required. Due to this, bone grafts are in high demand in several countries as an advanced solution for bone disorders.

Despite many advances in the past few decades, the treatment of critical-sized bone defects remains a significant concern, and there is a clinical need for improved therapeutic strategies. In the current treatment of bone repair, standard bone-grafting approaches such as autogenic, allogenic, or xenogenic grafts are used. Autologous bone graft is considered the “gold standard” among them because of its osteogenic, osteoinductive, and osteoconductive potential [5]. Compared to the autografts, allografts and xenografts have limited clinical success due to the potential of disease transmission and immunological rejection [6]. Nevertheless, autografts show several drawbacks, such as donor site morbidity, scarce supply of healthy tissues, and costly surgery, severely restricting their use. These limitations have prompted research in alternative bone grafting approaches and synthetic bone grafts have developed as a potential therapeutic choice for treating bone disorders and reconstructing bone defects [7].

Since then, traditional processing techniques have been utilized to fabricate many biomedical scaffolds that provide a proper microenvironment for the attachment and proliferation of cells, fulfilling all criteria for an ideal scaffold [8]. Ideal bone grafts must fulfill specific requirements, including biocompatibility, appropriate structural, functional, and mechanical properties that mimic native bone and do not elicit adverse immunological reactions [9]. Traditional processing techniques have been utilized to fabricate a number of biomedical porous implants or scaffolds. Such porous scaffolds provide a proper microenvironment for the attachment and proliferation of bone cells, fulfilling all the criteria for an ideal scaffold [8]. However, conventional fabrication techniques remain a source of considerable concern due to their inadequacy at producing customizable shapes to meet specific patient needs [10].

Three-dimensional (3D) printing, also known as additive manufacturing, has led to a striking revolution in medicine and biology by enabling the production of customized implants and scaffolds [11]. The success of 3D printing in fabricating bone scaffolds primarily relies on its ability to create versatile constructs with precise, complex, and customized geometry entirely through computer-aided design (CAD) based on a patient’s MRI (magnetic nuclear resonance) or CT (computed tomography) scan, eliminating the need for part-specific tooling [10]. Further, additive manufacturing technology decreases processing time for low-volume production and reduces raw material waste. 3D printed bone grafts often possess extremely precise and sophisticated macro- and microstructures, which are key requirements for synthetic constructs; however, they rarely provide the desired ‘functionality’ equivalent to the native host tissue. The function of novel 3D printed scaffolds should not be limited to providing adequate mechanical and structural support but needs to be extended to deliver biological signals to guide and direct tissue regeneration.

Recent advances in 3D printing also enable the introduction of biomolecules in extremely precise, spatially predefined locations for localized targeted therapy in bone disorders. Various pathological conditions disrupt the equilibrium between bone-forming osteoblast and bone-resorbing osteoclast cells. While a number of pharmaceutics are available to treat bone disorders, oral administration of drugs has limited therapeutic efficacy due to the high volume of distribution and low drug concentration at the desired tissue site. Consequently, higher pharmacological dosages are required to achieve therapeutic effects, frequently resulting in adverse side effects and unnecessary accumulation in non-target tissues, leading to cytotoxicity [12]. To address these challenges, researchers have proposed a localized drug delivery system to treat bone disorders by incorporating active pharmaceutical and biological agents directly within bone scaffolds. During the past decade, targeted therapy has contributed to considerable progress in bone disease treatment by controlling pathological reactions and improving device function [13,14]. Integration of adequate doses of different biological agents within complex 3D matrices further enhances the functionality of these scaffolds [15]. For example, one study reported that a recombinant human bone morphogenetic protein 2 (rhBMP-2) eluting 3D printed PCL/β-TCP scaffold was evaluated for osteogenesis efficiency in critical size defects of *in vivo* sheep models [16]. The collagen sponge loaded with rhBMP-2 on a 3D printed scaffold increased the overall volume of new bone tissue growth compared to the control group.

The use of natural medicinal compounds (NMCs) in bone tissue engineering has the potential to be a safer and more effective alternative to synthetic drugs, with potentially fewer and less severe side effects. Osteogenic, antibacterial, anti-inflammatory, and anticancer properties of natural herbal medicines make them a potential option for preventing infection, reducing inflammation, and inducing apoptosis of cancer cells, while promoting bone formation [17–20]. Researchers have studied the use of compounds such as curcumin and *aloe vera* gel extracts in bone tissue engineering applications because they stimulate new bone growth [21,22]. Functionalizing 3D printed scaffolds with natural biomolecules that possess osteogenic, angiogenic, anticancer, and antibacterial properties is a promising approach for addressing musculoskeletal disorders.

In this review, we will discuss the current advances and critical concerns in localized drug delivery based on different 3D printed biomaterials. Here, we focus on potential and promising applications of novel drug delivery vehicles incorporated with NMCs from 3D printed scaffolds to treat various bone disorders (Fig. 1). We will then discuss effective strategies for drug loading and release in terms of possible drug-material interactions. These strategies may guide researchers toward the effective design, fabrication, and implementation of these multifunctional scaffolds for various bone disorders. We hope this review offers new insights toward developing novel functional 3D printed scaffolds, which may provide the localized delivery of specific NMCs to treat bone-related disorders and promote bone regeneration simultaneously.

## 2. Common bone disorders and the use of natural medicinal compounds (NMCs)

### 2.1. Osteoporosis and NMCs with Osteogenesis properties

Abnormalities in bone remodeling can cause various skeletal disorders, among which osteoporosis is the most common metabolic bone disorder associated with low bone mass and deterioration of microarchitectural bone tissue. Older people are more vulnerable to osteoporosis due to increased bone resorption induced by low levels of parathyroid hormone and calcitonin. Moreover, osteoblast or bone-forming cells become less active, and calcium absorption decreases at older age. Some inevitable genetic factors such as petite body frame, family history, race, and gender can be linked to a higher risk of developing osteoporosis. Prolonged exposure to certain medications, including corticosteroids, heparin, cytotoxins, anticonvulsants, and cyclosporine, may be associated with osteoporosis.

Various anti-osteoporotic medications have been approved to treat osteoporosis and osteoporotic-related fractures. However, patients and medical advocates are concerned about the safety and efficacy of anti-osteoporotic drugs over time. Bisphosphonates, a group of drugs approved by the FDA to treat osteoporosis, reduce osteoclastic bone resorption at bone remodeling sites. However, bisphosphonates, such as alendronate, ibandronate, risedronate, and zoledronic acid, showed serious and worrisome side effects within a year of its launch, including an increase in bone fragility or bone fractures in patients. Calcitonin is the hormone that inhibits osteoclast activity by binding to the calcitonin receptors in osteoclasts and, therefore, reduces bone resorption. However, this polypeptide hormone produced by the thyroid gland has various side effects, including flushing, nausea, vomiting, and diarrhea. Anabolic agents increase the number of both osteoblast and osteoclast cells, resulting in increased bone density. Side effects of anabolic agents include male characteristics in women and liver toxicity.

Scientists have been searching for safer alternatives to osteoporosis medications due to their long-term side effects and limited efficacy for osteoporotic fractures. The therapeutic components found in herbal plants are effective in preventing and treating osteoporosis. A regular diet rich in fruits and vegetables with higher amounts of vitamin C, magnesium, potassium, and beta carotene contributes to increased total bone mass, which supports osteoporosis treatment. Calcium and vitamin $D_3$ supplements also reduce fractures and strengthen bones.

Herbal medicines can prevent or alleviate osteoporosis symptoms by acting on the bone cells, inhibiting inflammation, reducing oxidative stress, and increasing estrogen hormone levels [23]. Herbal medicines also increase bone density while decreasing bone resorption. The phytoestrogens produced naturally by plants increase intestinal calcium resorption, decrease calcium excretion, and promote calcitonin synthesis. In addition, NMCs inhibit the production of proinflammatory cytokines, which contribute to osteoporosis and bone loss. The antioxidant capacity of NMCs scavenges free radicals, reducing the expression of cyclooxygenase-2 (COX-2) and tumor necrosis factor α (TNF-α). The reduction of COX-2 and TNF-α expressions reduces osteoclast activity by reducing the production of

the receptor activator of NF-ligand (RANKL). Table 1 shows the various NMCs that have demonstrated promising effects on bone regeneration.

### 2.2. Osteomyelitis and NMCs with antibacterial properties

Osteomyelitis is generally defined by bacterial infection-induced bone and bone marrow inflammation. Despite being one of the oldest diseases of humankind, the pathophysiology and treatment regimens of musculoskeletal infections are relatively unexplored. Even with the advances in antibiotic therapy, sterility of implant sites, and aseptic surgical treatments, the incidences and socio-economic burdens of osteomyelitis are still on the rise.

Based on the mechanism by which it begins, bone infections can be classified into two broad categories: endogenous seeding and exogenous seeding. Endogenous seeding, also known as hematogenous infection, is mainly caused by bacterial transport through the bloodstream, and children are predominantly affected by it. The most common exogenous bacterial inoculations are generally caused by an adjacent fracture site and also include infections from prosthetic devices or surgical tools. Once orthopedic scaffolds are implanted in the physiological system, they function as foreign materials, making them susceptible to microbial infections. Early-linked revisions of total knee arthroplasty (43.9%) and total hip arthroplasty (21.5%) are both most commonly caused by prosthetic joint infection (PJI). These infections can appear anytime after surgery and are categorized as early, delayed, and late prosthetic joint infections (PJI). Early infection (<3 months) is caused by the introduction of highly virulent bacteria at the time of surgery. Delayed infection (3 months-2 years) is also acquired at the time of operation but is caused by less pathogenic microbes. Late infection (>2 years) is mainly caused by hematogenous infection [31].

Osteomyelitis is classified as either acute or chronic, based on the duration of the infection [32]. Acute infections that evolve over several days to a few weeks are mainly characterized by inflammatory changes in the bone. Acute infections can be easily cured with antibiotic therapy. Chronic osteomyelitis relapses and persists over several months to years and is mainly characterized by necrotic bone. Treatment of osteomyelitis includes surgical debridement followed by appropriate antibiotic therapy for at least 4–6 weeks. Approximately 75% of all osteomyelitis is caused by bacterial pathogens in the genus Staphylococcus, among which the *Staphylococcus aureus (S. aureus)* strain is responsible for 30–60% of implant-related infections [33]. The ability to form biofilms, resist antimicrobial agents, and secrete a toxin that eliminates host defenses makes *S. aureus* an extremely virulent pathogen. Other microbial species that cause osteomyelitis are *Escherichia coli* (in the *Enterococcus* family), *Pseudomonas* such as *Pseudomonas aeruginosa (P. aeruginosa)*, and *Streptococcus*. Ticarcillin/clavulanate and fluoroquinolone are the preferred antibiotic therapies for Enterobacteriaceae, whereas cefepime and piperacillin/tazobactam are the top choices for *P. aeruginosa* infections [34].

In the case of implant-associated osteomyelitis, antibiotic-impregnated bone cement has been used to repair the defect created by surgical removal of the infected implant and nearby bone and tissue [35]. Nevertheless, antibiotic resistance and antibiotic-induced mechanical strength deterioration are major concerns. Antibiotic resistance is increasing due to widespread antibiotic usage and abuse and the stagnation in discovering novel antibiotics.

However, plant-derived NMCs can combat the rise of antibiotic resistance. NMCs are promising alternative antibiotic sources because they have several mechanisms of action against bacteria, easy availability, and proven pharmaceutical effectiveness. Antivirulence activities of NMCs can avoid resistance by targeting bacterial virulence and nonessential cellular process [36]. The actions against bacteria reduce the development of resistance toward NMCs, maintain novel antibacterial action mechanisms of NMCs, and enhance the effectiveness of pharmacological agents against bacteria [37]. In addition, 50% of FDA-approved antibacterial agents are from plants [38]. The use of medicinal herbs to treat infection is common, and a growing body of evidence has shown that using NMCs alone or with other antibiotics can arrest bone infection-causing bacteria, as described in Table 2.

### 2.3. Osteosarcoma and NMCs with chemopreventive properties

Osteosarcoma has early metastasis, poor prognosis, rapid progression, and a high degree of malignancy. It is estimated that 4.4 people per million in the United States are diagnosed with osteosarcoma each year, representing for less than 1% of all cancers diagnosed in adults [46]. It is the third most frequent primary malignancy among children and young people. Typically, osteosarcoma occurs in the lower extremity metaphysis of long bones among adolescents, however this is not the case in older patients. The incidence of craniofacial and axial osteosarcoma continues to rise with age, contributing for 40% of all occurrences beyond the age of 60 [47].

Before the mid-70s, amputation was the mainstay for osteosarcoma treatment, with an extremely poor survival rate of 20%. Adjuvant chemotherapy, introduced in the 1970s, boosted the five-year survival rate for osteosarcoma patients to 50% [48]. By 1990, the conventional treatment had shifted to a new combination of neoadjuvant and adjuvant chemotherapy and surgery, which increased the survival rate to more than 65% [48]. However, current studies have revealed that this rate appears to have plateaued for the last two decades, even with the introduction of combined chemotherapy.

Nowadays, osteosarcoma patients receive pre-surgical chemotherapy, which helps to decrease the tumor size before a surgical resection of the entire volume of diseased tissue and a post-operative chemotherapeutic regimen [49]. After pathological diagnosis, standard chemotherapeutic drugs including doxorubicin, ifosfamide, cisplatin, and high doses of methotrexate are administered and continued for 6–10 weeks, prior to local control. Surgical options can be either limb salvage or amputation. Limb salvaging chemotherapy is considered a safe treatment strategy for 85–90% of patients with severe osteosarcoma. To avoid recurrences, resection eliminates the area of diseased tissue with at least a 2 cm margin. Amputation, once considered to be the standard surgical treatment for osteosarcoma, is now reserved for only non-resectable tumors in soft tissue. Chemotherapy is restarted within 2–3 weeks of surgery once the incision is healed [50].

Osteosarcoma survival rate has been unchanged over the past three and a half decades, although combined chemotherapy has been introduced [51]. The most concerning factors include complications and incidences of fatal toxicity related to high doses of chemotherapeutic agents, such as methotrexate [52]. The common side effects include gastrointestinal reactions and myelosuppression, which typically manifests as decreased

bone marrow activity, resulting in reduced production of blood cells. Recent studies have also shown that high doses of chemotherapeutic agents show no advantages over less toxic moderate dosages in terms of survival rate. The main side effects of doxorubicin are cardiotoxicity, and the incidence of heart failure increases with high doses of adriamycin therapy [53]. Cisplatin is associated with major concerns, including peripheral neuropathy, hearing loss, kidney damage, and hypomagnesemia, while the most severe side effects of ifosfamide include bladder toxicity.

Indeed, therapeutic compounds derived from natural sources are used in the current treatment of osteosarcoma [54]. Herbal medicines are often more desirable than synthetic drugs since their extracts contain various pharmaceutical compounds such as flavonoids, phenols, and other secondary metabolites. NMCs are also less toxic to humans and bring in synergistic anticancer effects [55]. The multitargeting ability of natural extracts influences multiple cellular pathways to regulate proteins, genes, and multiple factors that induce apoptosis in cancer cells and boost immune system action against cancer cells [55,56]. NMCs have been investigated for their efficacy in inducing osteosarcoma cell death through different pathways, as presented in Table 3.

### 2.4. Osteoarthritis and NMCs with anti-inflammatory properties

Osteoarthritis is one of the primary causes of global disability, affecting approximately 250 million people worldwide [66]. The degenerative joint disease can cause joint locking, severe pain, stiffness, or loss of flexibility. As the world's population ages and the frequency of obesity rapidly rises, the socioeconomic burden and substantial health costs related to osteoarthritis continue to increase dramatically. For a long time, osteoarthritis was viewed as a simple degenerative "wear and tear" disease, limited to the degradation of articular cartilage; consequently, the pathophysiology of the disease and the development of diagnostic tools were severely neglected. However, in recent years, new insights have revealed osteoarthritis to be a joint disease, and researchers have prioritized the search for new treatments in light of its status as a disease.

The pathogenesis of osteoarthritis is a complex process involving mechanical, inflammatory, and metabolic factors that ultimately destroy articular cartilage, inflammation in the synovium, osteophyte formation, and bone hypertrophy. As the largest synovial joint, the knee is the most frequent site for painful osteoarthritis, accounting for roughly 85% of osteoarthritis cases, followed by the hip and hand [67].

Current management for osteoarthritis falls into three broad categories based on a comprehensive assessment of the severity and the patient's lifestyle: 1) personal lifestyle modifications or the non-pharmacological approach 2) pharmacological, and 3) surgical interventions. Basic treatment of osteoarthritis starts with educating and encouraging patients to exercise regularly and adopt a healthier lifestyle by quitting smoking, limiting alcohol consumption, and maintaining a proper sleeping and diet regime. The next level of treatment includes providing patients with expert advice from physiotherapists on weight loss training and physical activities such as aerobic exercise, swimming, cycling, and elliptical training. Bracing, splinting, and the usage of a cane are other non-pharmacologic

treatments that can help patients with painful joints continue daily activities and reduce osteoarthritis symptoms [68].

Acetaminophen can be used as a pharmaceutical therapy for mild osteoarthritis. It is effective and low-cost drug with less gastrointestinal side effects than nonsteroidal anti-inflammatory drugs (NSAIDs) [69]. NSAIDs such as diclofenac, ibuprofen, and naproxen, are prescribed as a second-line treatment when the symptoms are moderate. However, they can cause serious side effects such as gastrointestinal bleeding, renal dysfunction, and high blood pressure.

As an alternative to NSAIDs, COX-2 inhibitors like celecoxib are used, which have similar efficacy as standard NSAIDs and may cause fewer gastrointestinal side effects. However, they are more expensive and elevate the risk of cardiovascular complications. If acetaminophen or NSAID therapy does not relieve a patient's symptoms, low doses of opioids are suggested. However, prescribing opioids introduces a high risk of patient drug abuse or addiction, requiring prescription drug monitoring programs (PDMPs). Patients with moderate to severe osteoarthritic pain may find short-term (1–2 months) relief with intra-articular corticosteroids. However, excessive use causes skin atrophy, dermal depigmentation, and severe cartilage destruction. Other treatments like intra-articular hyaluronic acid derivatives, nutraceuticals such as glucosamine and chondroitin sulphates, and topical capsaicin have generated several controversies, either about their efficacy or related adverse effects, and are thus not recommended [70,71].

Herbal medicines have been studied as an alternative anti-inflammatory compound to reduce the toxicity and side effects of NSAIDs [72]. NMCs suppress the function of chemokines, cytokines, and adhesion molecules. They also inhibit arachidonic acid and nitric oxide pathways [73]. However, just like any other medicinal compound, interactions between active compounds should be considered, and consult physicians if there is any concern. NMCs effectively repair osteoarthritis-related bone fractures by controlling inflammatory cytokine productions, as described in Table 4.

## 3. Strategies of natural medicine delivery from biomaterials

NMCs have shown efficacy for treating a variety of bone diseases. However, their bioavailability is heavily compromised due to its high degradation in physiological environment. In addition, many of these compounds exhibit nonpolar/hydrophobic properties, limiting their potential in controlled release systems. Various novel drug delivery carriers synthesized from organic and inorganic materials have been introduced to address drawbacks that limit their clinical applications. Innovative drug delivery vehicles can improve drug efficacy by approaching targeted sites, enhancing drug permeability, and improving stability and bioavailability while reducing cytotoxicity. These delivery vehicles also modulate drug release kinetics to achieve sustained release for long-term treatments. In this section, we focus on advanced drug delivery systems and their applications for bone tissue engineering.

## 3.1. Lipid-based drug delivery systems

**3.1.1. Liposomes—**Liposomes are sphere-shaped vesicles comprising phospholipid bilayers enclosing an aqueous compartment. This distinctive structure provides liposomes with a unique ability to incorporate both hydrophobic and hydrophilic pharmaceutical agents, where shell-like phospholipid bilayers provide housing for the hydrophobic drugs within the membrane and hydrophilic molecules are typically entrapped within the aqueous core [80]. Liposomes are extensively employed as drug delivery systems because of their ability to: alleviate undesired tissue-toxicity, protect the encapsulated drug from external environments and enhance drug stability, allow targeted site-specific delivery, and control release kinetics. Our group fabricated liposomal curcumin, incorporated within 3D printed calcium phosphate scaffolds with a designed shape and porosity [81]. Encapsulation of curcumin into liposome enhanced its bioavailability and exhibited sustained release of curcumin from the bone scaffold. Liposomal curcumin released from 3D printed scaffold showed cytotoxicity toward osteosarcoma cells, while it promotes osteoblast cell attachment, viability, and proliferation.

## 3.2. Polymer-based drug delivery systems

**3.2.1. Polymeric Micelles—**Micelles are self-assembled nano-constructs formed by amphiphilic polymers that arrange their hydrophobic end toward the inner core and point the hydrophilic section outward to form a core-shell structure [82]. Above critical micelle concentration (CMC) and critical micelle temperature (CMT), the hydrophobic segments form a hollow core which entraps the non-polar drugs, thus enhancing their water solubility and bioavailability. Micelles are excellent drug carriers because of their unique properties, including high drug loading capacity, non-toxicity, ease of modification, biocompatibility, and controllable drug release kinetics. A self-assembled curcumin-loaded micelle using alendronate-hyaluronic acid-octadecanoic acid was fabricated to enhance the therapeutic efficacy of curcumin on osteosarcoma [83]. Sustained release from micellar curcumin exhibited higher cytotoxic activity against MG-63 osteosarcoma cells and slowed tumor growth in osteosarcoma-bearing mice, compared to free curcumin. Micelles also have challenges in drug delivery applications, such as the risk of premature drug leakage and instability in blood circulation. To address these limitations, surface modification of the micelles is often carried out.

**3.2.2. Polymeric nanoparticles—**Polymeric nanoparticles are solid colloidal particles ranging in size from 1 to 100 nm. They have gained popularity as drug carrier candidates owing to their straightforward drug-loading procedures, which include incorporation and entrapment of drug molecules during nanoparticle formulation, adsorption of drug molecules after nanoparticle formation by incubation in a drug solution, or chemical conjugation of therapeutic molecules into the nanoparticle matrix [84]. Polymeric nanoparticles also have favorable properties in terms of their large surface area with surface functional groups, which allow for site-specific target delivery, excellent biodegradability, biocompatibility, and the ability to modulate size and size distribution as well as controlled release kinetics [85]. A study showed that nanoparticle-encapsulated curcumin exhibited synergistic effects with antibiotic ciprofloxacin to inhibit the growth of *Pseudomonas aeruginosa* by downregulating mexX and oprM gene expressions [86]. This study shows curcumin promotes bacterial cell

death and can be used with other antibiotics to improve their efficacy and reduce bacterial resistance. Polymeric nanoparticles also have some limitations as drug delivery carriers, including risks of toxicity due to the use of PVA during synthesis, and difficulty with scaling up.

**3.2.3. Hydrogels—**Hydrogels are networks of hydrophilic cross-linked polymers capable of swelling while absorbing a significant amount of water and shrinking while facilitating controlled drug release. Drugs are loaded into hydrogels during either the polymerization or sol-gel transition stage when the polymer chains absorb a high-concentration aqueous drug solution [87]. Hydrogels have excellent biocompatibility due to their highly porous structure and high water content, similar to physiological tissue. These properties allow effective drug loading into the gel matrix, controlled biodegradability for subsequent drug release, and responses to stimuli such as physical, chemical, and biological changes, ultimately making them a potential platform for drug delivery purposes [88]. A recent study exhibited the fabrication of quercetin-bioglass sodium alginate injectable hydrogel for articular cartilage repair. The hydrogel improves the bioavailability of quercetin, upregulates genes that maintain chondrocyte phenotype, and reduce inflammatory response by promoting M2 macrophage polarization [89]. However, as drug delivery vehicles, hydrogels have drawbacks such as insufficient mechanical properties, limited loading capacity for hydrophobic drugs, and rapid drug release due to large water content and high porosity.

### 3.3. Inorganic drug carriers

**3.3.1. Mesoporous silica—**Mesoporous silica is an inorganic nanoconstruct characterized by a uniform and ordered arrangement of mesopores (pore size 2–50 nm) within an amorphous silica matrix. Mesoporous silica exhibits a honeycomb-like porous structure into which functional and therapeutic agents can be loaded by diffusion mechanisms; the resulting load capacity is high due to high pore volume and the large and active surface area [90,91]. Mesoporous silica can also provide target-specific drug delivery by either introducing surface modifications or incorporating magnetic materials, both without causing cytotoxicity. Another advantage of mesoporous silica, which has attracted considerable attention for drug delivery purposes, is its drug release kinetics, which can be easily tailored due to the narrow distribution of pore sizes and tunable pore diameters. Curcumin-loaded mesoporous silica within a chitosan film has been fabricated to improve functional properties of chitosan food packaging film [92]. pH-responsive and sustained release of curcumin from mesoporous silica demonstrated efficient antimicrobial activity against *Escherichia coli* and *Staphylococcus aureus.* The major drawbacks of mesoporous silica include premature drug leakage, melanoma promotion, and hemolysis caused by an adverse interaction between the surface silanol groups of mesoporous silica and phospholipid groups present in the red blood cell membrane.

**3.3.2. $TiO_2$ nanotubes—**Titanium oxide nanotubes (TNTs) are electrochemically fabricated oxide layers on titanium implant surfaces. Parameters of the anodization process, such as voltage, time, and electrolyte type, can control the dimensions of TNTs [93]. Owing to their high total surface area, enhanced wettability, good biological wear resistance,

antibacterial features, and their potential to act as drug delivery vehicles, TNTs became popular in bone tissue engineering. However, the critical challenge of TNTs as a drug delivery system is their uncontrolled drug release kinetics. To improve the benefits of nanotubes, several studies have investigated the effects of biodegradable coatings and surface modifications designed to modulate the drug release kinetics. The direct-drop method has been employed to coat curcumin onto $TiO_2$ nanotubes formed on and around Ti6Al4V implant surface for orthopedic applications [94]. Results indicated that curcumin coated nanotubular surface demonstrated antibacterial properties against *Escherichia coli* and *Staphylococcus aureus* within 24 h. While the curcumin coated $TiO_2$ nanotubes did not show cytotoxic effects on human mesenchymal stem cells, it increased cell proliferation, and induced *in vitro* osteoblast differentiation by upregulating alkaline phosphatase expression.

### 3.4. Biomimetic/bioinspired drug delivery systems

**3.4.1. Exosomes—**Exosomes are membrane-bound extracellular vesicles ranging in size from 30 nm to 150 nm [95]. Their primary function is facilitating intercellular communication by transporting biomolecules, including ribonucleic acids (RNAs), deoxyribonucleic acids (DNAs), proteins, and lipids. Exosomes are extensively used as drug delivery systems for their outstanding advantages, including long-term stability, high drug loading capacity, target selectivity, low immunogenicity, and enhancing drug solubility [95]. An *in vivo* study showed osteoblast-derived bio vesicles **enhance osteogenesis** [96]. The exosomes secreted by mineralizing osteoblasts were shown to activate the Wnt/−catenin pathway, which in turn induced the osteogenic differentiation of bone marrow stromal cells (ST2 cells) in an *in vitro* study [97]. Osteoclast-derived exosomes containing RANK inhibit *in vitro* osteoclastogenesis by binding to RANKL in the bone microenvironment [98].

## 4. Mechanism of drug loading on bone scaffolds

To date, the focus of conventional bone scaffolds has been primarily aimed at providing structural support for regenerating or replacing bone tissue, whereas future bone grafts aim at designing and constructing “functionalized scaffolds” that not only help in bone-tissue regeneration but also simultaneously treat various bone-related disorders. 3D printed bone scaffolds with controlled porosity enable the achievement of the appropriate mechanical and biological properties for bone tissue engineering. Such 3D printed bone scaffolds can be combined with NMCs and/or NMCs with nano or micro-sized drug delivery carriers to provide a localized drug delivery system, potentially enhancing bone healing, and reducing post-implantation problems. Numerous *in vitro* and *in vivo* studies have shown that scaffold-based local drug delivery systems enhance bioavailability and the sustained delivery of biomolecules while alleviating tissue toxicity. Incorporating drug molecules into 3D scaffolds is achieved by the following methods: physical entrapment, unspecific adsorption, physisorption, and chemisorption. In the case of physical entrapment, biomolecules or pharmaceuticals are incorporated within the 3D printed scaffolds during manufacturing. Other drug-loading strategies, such as unspecific absorption, physisorption, and chemisorption, have been introduced to address this challenge. These methods allow the incorporation of a variety of drug molecules without compromising their pharmacological efficacy. It is worth mentioning that most non-porous metallic scaffolds cannot absorb

pharmaceuticals and thus require a polymer or ceramic coating before drug loading to achieve successful drug loading and the gradual release of the drug [99]. This section focuses on effective strategies for incorporating drugs into metal, ceramic or polymeric scaffolds for various bone tissue engineering applications. Various drug loading and drug release mechanisms are shown in the schematic illustrations found in Fig. 2.

### 4.1. Physical entrapment

Physical entrapment is a popular drug loading method in which therapeutic molecules are physically enclosed within the 3D biomaterial matrix during the synthesis of the scaffold. The therapeutic drug molecule or biologically active substance is physically mixed with the biomaterials before scaffold fabrication. A favorable interaction between the drug and the biomaterial is essential for homogeneous drug distribution and high drug loading efficiency [100]. The scaffolds can be fabricated using the prepared drug-materials mixture in a 3D printer at mild temperatures [101]. Although therapeutic molecules for enhancing bone regeneration can be physically entrapped in 3D printed scaffolds with an appropriate porous structure, this approach results in low surface resolution of the printed parts. The main advantage of physical entrapment is a lower risk of loss of activity of the drugs since no harsh chemicals are used. However, high printing temperatures limit the available drugs to those that can withstand unfavorable processing environments.

Several studies demonstrate that natural medicinal compounds can be physically entrapped in 3D scaffolds and tested for their biological properties. One such study found that poly (lactic acid)/nanohydroxyapatite composite scaffolds embedded with *Equisetum arvense* extract (EE) improved *in vitro* biological properties [102]. Due to the accumulation of EE on the surface, the scaffold shows an initial fast release of EE, followed by a sustained release for three weeks. *In vitro* release of EE enhanced proliferation and cell attachment of human adipose tissue-derived mesenchymal stem cells (AT-MSCs). It also induced *in vitro* osteogenic potential by increasing ALP activity and mineralization.

In another study, human umbilical cord-derived mesenchymal stem cells loaded on a PCL-graphene oxide (GO)-*Cissus quadrangularis* (CQ) scaffold showed enhanced bone regeneration compared to control samples in *in vivo* rat models. This result demonstrated the synergistic effect of GO and CQ on new bone formation in the defect site [103]. A recent study confirmed the potential for biomedical applications of *aloe vera*-embedded, cellulose nanofibril-reinforced bio-hydrogels deposited by direct ink writing [104]. The 3D structures of this application were precisely printed without shrinkage or swelling because their mechanical properties had been improved by the uniform dispersion of 2,2,6,6-tetramethylpiperidin-1-oxy-oxidized cellulose nanofibers within a system that showed strong hydrogen bonds interactions.

### 4.2. Unspecific adsorption

In unspecific adsorption, a drug solution is adsorbed and immobilized on the surface of a 3D printed scaffold without any physical or chemical interaction forming between the drug particles and the biomaterials. Numerous studies have reported successful incorporation of therapeutic molecules into 3D scaffolds by unspecific adsorption [105,106]. The drug-

loading ability of unspecific adsorption is mainly determined by the structural parameters of the scaffold, including the specific surface area (SSA) and porous architecture [105].

SSA is defined as the ratio of the total surface area of the material to its mass, and it is directly related to the quantity of therapeutic molecules absorbed in the scaffold. One study reported that changing the SSA value from 11 to 88 $m^2 \cdot g^{-1}$ leads to a 14-fold increase in the adsorption of cytochrome *c* on HA particles [107]. Pore architectures, such as total porosity, pore interconnectivity, pore size distribution, and pore shape, are additional parameters that determine drug loading efficiency [108]. Increased scaffold porosity results in a higher surface area, which improves the drug loading efficiency. The total porosity is linearly related to the quantity of drug embedded on a biomaterial surface. For example, a study showed that increasing the total porosity of β-TCP beads from 20 to 40% improved vancomycin adsorption by up to 200% [109].

Another study found that microporous HA enhanced the adsorption efficiency of vancomycin, gentamicin, and ciprofloxacin antibiotics compared to dense HA [110]. Similarly, ampicillin and cytochrome *c* adsorption were 5- and 10-fold greater, respectively, on 3D printed PLA scaffolds with micropores compared to dense scaffolds [105].

### 4.3. Physisorption

Physisorption or physical interaction is another driving force often used to immobilize biologically active substances or drugs in the scaffold carrier. In physisorption, drug molecules are adsorbed on scaffold surfaces by hydrogen bonding, van der Waals forces, electrostatic, hydrophobic, or hydrophilic interactions with biomaterials [111,112].

Unlike nonspecific absorption, electrostatic interactions between polar drugs and the charged surfaces of biomaterials allow the surfaces to have a higher affinity and enhanced drug loading ability. For example, a study investigated the loading efficiency of cisplatin in two different nano-structured hydroxyapatite (HA) carriers: plate-shaped HA nanocrystalline material (HAps) and needle-shaped HA nanocrystalline material (HAns) [112]. Although HAns has a lower surface Ca/P ratio than HAps, the more negatively charged surface of HAns resulted in a more favorable electrostatic binding with positively charged hydrolyzed cisplatin and exhibited higher drug loading efficiency than the uncharged Haps's surface. The loading efficiency of growth factors, such as BMP-2 and VEGF, was also enhanced by introducing a negative charge on the surface of the scaffold [113].

Another form of physical interaction between biologically active molecules and the scaffolds are hydrophobic and hydrophilic interactions. Generally, hydrophobic molecules in drug solutions attach more favorably to the hydrophobic surfaces of the scaffold. In contrast, hydrophilic interaction between drugs and the scaffolds can restrict drug loading capacity due to the increased interface phase tension between the drug solution and the scaffold surface [114]. For example, one study showed that increasing the hydrophobicity of HA scaffold led to improved adsorption affinity for hydrophobic lysozyme [115]. However, hydrophilic HA carriers showed low drug loading efficiency for highly water-soluble drugs such as riboflavin sodium phosphate and metoprolol tartrate [114].

While physisorption is a simple and effective method of drug loading, it can restrict the loading efficiency due to weak interactions and result in undesired drug release.

### 4.4. Chemisorption

To overcome the limitations of physisorption, covalent interactions or chemisorption has emerged as a promising approach to drug loading in scaffolds. In chemical adsorption, the binding between drug molecules and biomaterials is obtained by covalent bonds. Although the drug is loaded at a slower rate in chemisorption compared to nonspecific adsorption or physisorption, this approach can prevent burst release due to the strong bonds between drugs and scaffolds. Other advantages of chemisorption are improved drug stability, homogeneous distribution of biomolecules in the scaffold matrix, and lower probability of drug aggregation.

The covalent bonding commonly occurs between phosphate, hydroxy, carboxyl, and amine groups of the scaffold biomaterials and the drugs. For example, alendronate was chemically adsorbed on biphasic TCP/CP (calcium pyrophosphate) through the ligand exchange [116]. Similarly, the zoledronate can be covalently linked to the surface of HA [117]. In the case of polymers, chemisorption can reduce unfavorable interactions between drugs and polymers. In addition, ibuprofen can be covalently linked to the carboxylic acid-functionalized polyethylene glycol scaffold [118].

Chemisorption did not gain considerable popularity due to the complexity of the procedure and high cost, yet this process allows a sustained and controlled drug release pattern from the scaffold at different environmental pH values.

## 5. Controlling drug release

In tissue engineering applications, controlled release can help to achieve long-term drug presence at clinically relevant concentrations at the local tissue site. However, an initial burst release of the drug is commonly observed right after the scaffold implantation at the defect site. The large porosity and high surface-area-to-volume ratio of the scaffold usually trigger the burst release of drugs. The initial burst release of osteogenic or antibiotic drugs is often desirable to enhance wound healing and promote immediate relief from bacterial invasion right after implantation [119]. In the case of chemopreventive drugs, an initial higher drug release event followed by sustained release from the scaffold helps to eradicate residual malignant cells in the surrounding tissue sections in case of post-osteosarcoma resection defect repair [21]. However, it can cause adverse effects and tissue toxicity if the local drug concentration exceeds the maximum therapeutic limit. In such cases, the amount of drug delivered by the burst release needs to be carefully monitored since failure to control the release often results in ineffective treatment and economically inefficient usage of drugs [119]. Thus, novel strategies such as controlling the porosity of the 3D printed scaffolds, modifying the drug-materials interaction, or applying a coating as a drug release matrix have been introduced to modulate the drug release kinetics. The ultimate goal is to develop localized drug delivery systems with well-maintained therapeutic drug concentrations delivered to target sites with minimal side effects on the surrounding cells and tissue [120].

Particularly, in the case of bone tissue engineering applications, controlled release of osteogenic drugs from 3D printed bone scaffolds has resulted in enhanced attachment, proliferation and differentiation of osteoblast or osteoprogenitor cells, which has led to improved bone regeneration and uncomplicated defect repair in animal models. [18,81,121–123].

### 5.1. Controlling pore architecture

Controlling pore structure is commonly used to manipulate the release kinetics. When comparing pore sizes, the presence of large pores promotes the initial burst release due to enhanced water adsorption and drug solubilization. In contrast, small pores result in sustained and long-term drug release because of the greater surface area available for drug adsorption than large pores [124]. A study that investigated the effects of pore size distribution on the release of antibiotics from hydroxyapatite microspheres found that a slower release of antibiotics was obtained by reducing the mean diameter of the hydroxyapatite microspheres from 0.82 to 0.53 um [125]. A recent study showed different release profiles of paracetamol from 3D printed polyethylene oxide (PEO) and ethyl cellulose (EC) polymeric scaffolds with different porosities [126]. Drug release increased 1.5 times in an acidic medium when the total porosity of the PEO scaffold changed from 28 to 61.7%. An increase in the total porosity of EC from 3.9 to 45.1% resulted in about a 6-fold increase in paracetamol released in the medium.

### 5.2. Controlling drug-material interactions

The interaction between a drug and the scaffolds that contain it is a crucial factor influencing the drug release kinetics. A study demonstrated that positively charged cisplatin on a negatively charged HA scaffold showed a slower drug release than from a neutral cisplatin complex [112]. In a similar study, formation of covalent bonding between a BMP-2-derived peptide and chitosan/HA scaffolds helped the peptide molecule to achieve zero-order release kinetics for a duration of 3 months. The peptide-loaded scaffolds also showed superior osteogenesis compared to scaffolds without the peptide [127].

### 5.3. Modifying coating materials

Calcium phosphates have been widely used as suitable coating materials in bone tissue engineering due to their superior bioactivity, bone composition similarity, and integrity with drugs. The controlled release of BMP-2 incorporated in a calcium phosphate coating on Ti disks yields enhanced osteogenic activity compared to the release of BMP-2 from uncoated Ti disks, which shows a burst release of the drug [128]. Antimicrobial peptides (AMPs) can be incorporated into Ti implants by creating titania nanotubes with a multilayer coating of CaP and a phospholipid coating. Sustained release of AMPs is achieved by the CaP- and phospholipid-coated Ti implant, which shows antibacterial activity with no cytotoxicity to osteoblasts and red blood cells [129]. Biodegradable polymer coatings on scaffolds have also been widely studied as the ideal delivery systems due to their non-toxicity, biocompatibility, biodegradability, and their ability to control drug release [130]. A recent study uses a PCL/PEG-coated CaP-based scaffold loaded with curcumin to enhance osteogenesis and inhibit osteosarcoma cell proliferation. Curcumin was incorporated into the PCL/PEG, which consists of FDA-approved bioresorbable polymers, to obtain the controlled release

kinetics. Curcumin in 3D printed TCP scaffolds showed osteogenesis effects and decreased proliferation of osteosarcoma cells [123]. Another recent study demonstrated that controlled vitamin $D_3$ release from 3D printed TCP scaffolds coated with a mixture of hydrophilic and hydrophobic polymers restricted osteoclast activity without showing cytotoxicity to osteoblast cells [131].

### 5.4. Tailoring spatiotemporal drug delivery

Despite many advancements, there are still challenges in delivering proper drugs at the different stages of bone healing to enhance therapeutic effects. One possible strategy for addressing these challenges is to introduce a sequential drug delivery system. Following bone trauma, wound healing and the bone regeneration process consist of the following phases: inflammation (0–3 days), proliferation (3–7 days), and remodeling (7 days-several months). Thus, the efficient delivery of drugs at the ideal time is essential to improving drug-mediated bone tissue engineering applications. Sequential drug delivery is being studied extensively to improve the bone healing process. A combination of BMP-2 and BMP-7 loaded on poly-electrolyte complexes of poly(4-vinyl pyridine) along with alginic acid microspheres have been investigated for use in sequential delivery [132]. The delivery system was designed to produce an initial higher release of BMP-2, followed by the slower release of BMP-7. This sequential approach improved osteogenesis differentiation of bone marrow-derived stem cells (BMSCs) compared to individual drug delivery systems. Another study of the sequential release of bone growth factors showed synergistic effects on the *in vitro* differentiation of BMSCs compared to a single BMP drug [132]. Similarly, the sequential release of dexamethasone and VEGF from PVA hydrogel/PLGA composites was studied for bone tissue engineering; the results showed that zero-order release of drugs from the composites was achieved over a 4-week period, which reduced inflammation and induced angiogenesis [133].

### 5.5. Controlling the printing process

The 3D printer’s layer-by-layer fabrication process can create a scaffold that modulates the release behavior of pharmaceutical molecules. During the 3D printing process, the drugs can be embedded in multilayer structures created from various materials. This technology results in the sequential release of drugs from the scaffolds. For example, diclofenac has been loaded into a 3D printed structure with two different polymer layers: Eudragit E 100, which degrades below pH 5.0, and Eudragit L 100, which degrades above pH 6.0. The embedded diclofenac demonstrated sequential release behaviors when pH levels were changed [134]. Layer-by-layer fabrication technology has also been used in bone tissue engineering. Isoniazid and rifampicin were each combined with a different binder and then alternately deposited in four layers, with a sequence of isoniazid-rifampicin-isoniazid-rifampicin. These isoniazid- and rifampicin-loaded 3D printed scaffolds achieved sequential drug release *in vitro* and *in vivo*, and exhibited no cytotoxicity toward rabbit bone marrow mesenchymal stem cells [135].

# 6. Current applications of 3D printed biomaterials for drug delivery

## 6.1. Ceramic 3D printed biomaterials as drug delivery vehicles to treat bone disorders

Ceramics have been researched as a viable dental and orthopedic implant materials owing to their better tissue responses [136]. Among all biocompatible ceramics, alumina ($Al_2O_3$) and zirconia ($ZrO_2$) are considered “bioinert” due to their minimal interaction with the host tissue. Bioinert ceramics were primarily employed for load-bearing prostheses and dental implants because of their high compressive strength and wear resistance. Alumina was chosen for such load-bearing applications because of its chemical inertness, high corrosion resistance, biocompatibility, and low wear rate. However, its low fracture toughness was a concern [136]. Zirconia ceramics have been widely used in dentistry and are still preferred as highly versatile materials for dental implants as well as for total hip and knee replacements. The major advantages of these zirconia-based materials are excellent biocompatibility, lower risk of allergic reactions compared to metals, excellent durability, excellent aesthetic properties (similarity to human teeth), the highest fracture toughness among similar classes of ceramics, and good corrosion resistance [137]. Unfortunately, these two ceramics have not proved useful as vehicles for drug delivery. In contrast to bioinert ceramics, calcium phosphate (CaP) ceramics, particularly hydroxyapatite (HA) and tricalcium phosphate (TCP), are widely considered to be desirable bone substitute materials due to their compositional similarities to bone, and their excellent bioactivity and bioresorbability [138,139].

Both physical and cell-mediated mechanisms in the physiological environment gradually dissolve bioresorbable CaPs. The solubility of CaPs in physiological conditions increases as the Ca/P ratio decreases. Solubility can also be increased by lowering crystallinity, density, and grain size. HA, $Ca_{10}(PO_4)_6(OH)_2$, is the most abundant mineral phase in bones and has a Ca/P ratio of 1.67. TCP, $Ca_3(PO_4)_2$, has two distinct phases: the α-phase and the β-phase. The solubility of α-TCP is higher than that of β-TCP. CaP ceramics function well in numerous bone tissue engineering applications as coating materials and bone fillers [140,141]. 3D CaP structures have drawn interest in bone defect repair in tissue engineering applications [142]. Recent developments in additive manufacturing have enabled the introduction of designed homogeneous porous architecture in HA and TCP scaffolds, which provides high surface area for the effective impregnation and controlled release of biologically active molecules [13]. Enhancing the functional properties of CaP scaffolds by biological or therapeutic functionalization is an emerging trend in bone tissue engineering.

Biological functionalization focuses on localized protein delivery, growth factors, or hormones that promote osteogenesis, angiogenesis, and cell proliferation and recruitment. However, therapeutic functionalization aims at treating various bone disorders or post-implantation pathologies such as osteosarcoma, osteomyelitis, and osteoporosis. It is worthwhile to mention that scaffold characteristics such as surface coating, microstructure, porosity, and specific surface area play a crucial role in the controlled release of the drug or biomolecule. These scaffolds quickly absorb and retain the active drug ingredient until they are implanted *in vivo* and then deliver the drug locally in a controllable manner over time,

as shown in Fig. 3 and Fig. 4. One of the earlier studies on drug delivery from bone tissue engineering scaffolds evaluated *In vitro* and *in vivo* biological properties of alendronate (AD) incorporated 3D printed TCP scaffolds (Fig. 3) [143]. To control the release of AD, a polycaprolactone (PCL) coating was applied to 3D printed TCP (Fig. 3A). Controlled AD release was achieved with a 1% PCL coating at pH 7.4 and pH 5.0 (Fig. 3B and C). Diffusion regulates AD release at pH 7.4, whereas TCP scaffold degradation dominates at pH 5.0; this difference in AD release regulation is demonstrated by $Ca^{2+}$ ion release in the medium and SEM images of the surface morphology of the scaffolds (Fig. 3D). Control TCP and PCL-coated TCP scaffolds at pH 5.0 release more $Ca^{2+}$ ions than control TCP at pH 7.4 buffer, indicating that TCP scaffolds degrade faster at the acidic pH, resulting in higher drug release. Hematoxylin and eosin (H&E) stained sections of AD-loaded TCP scaffolds with PCL coating (TCP + PCL + AD) showed significantly increased new bone formation 6 weeks after implantation compared to control TCP and PCL coated TCP (TCP + PCL) scaffolds. Optical microscopy images of H&*E*-stained sections from TCP + AD + PCL and TCP + AD show that PCL coating promotes new bone growth by preventing initial burst release and achieving sustained release (Fig. 3E). In another set of experiments, our group demonstrated that the controlled release of curcumin from 3D printed ceramic scaffolds increases new blood vessel development and new bone formation (Fig. 4) [123]. At pH 5.0 and 7.4, PCL/polyethylene glycol (PEG) coating releases curcumin at a higher rate than PLGA/PEG coating and no polymer coating. PCL/PEG coating increases the hydrophilicity of curcumin, resulting in enhanced aqueous solubility (Fig. 4B). Faster polymer coating degradation at pH 5.0 than at pH 7.4 leads to increased curcumin release in an acid environment (Fig. 4C). The curcumin-loaded TCP scaffold with PCL/PEG (Cur coated TCP) significantly enhances osteoid formation and mineralized bone, as shown after 6 weeks (Fig. 4D). Cur coated TCP also increases new blood vessel development compared to the control, indicating that curcumin promotes angiogenesis in the defect site (Fig. 4E).

In general, *in vivo* scaffolds are gradually degraded and replaced by new bone. Additionally, the high affinity of ceramics for drugs and proteins also assists in the convenient loading of biomolecules [13]. The drug release from ceramic scaffolds primarily follows two mechanisms: diffusion of biomolecules *via* the porous structure of the scaffold and through controlled degradation. *In vivo* and *in vitro* results have shown that 3D printed ceramic scaffolds incorporated with therapeutic molecules enhance new bone growth and angiogenesis, as shown in Fig. 5. Miao et al. demonstrated that dopamine-coated 3D printed β-tricalcium phosphate (β-TCP) scaffolds loaded with melatonin were able to stimulate osteogenesis [144]. The presence of melatonin improved the viability and proliferation of bone mesenchymal stem cells. MT-DOPA/β-TCP also facilitated more new bone growth in *in vivo* studies with the Sprague Dawley rat model than any other combination, such as β-TCP, DOPA/β-TCP (dopamine-modified β-TCP), and MT- β-TCP (β-TCP decorated with melatonin). Another study also reported that introducing vascular endothelial growth factor (VEGF) encapsulated in chitosan/dextran sulphate particles on 3D printed calcium phosphate cement scaffolds improved cell attachment and the proliferation of human dermal microvascular endothelial cells [145]. Calcium-phosphate-based scaffolds (CPC) incorporated with growth factor were fabricated by 3D plotting (Fig. 5A). The calcium phosphate cement scaffold showed cracks after immersion in water for 3 days, whereas

no crack formed when the scaffold was held in a humid atmosphere for 3 days (Fig. 5B). Confocal laser scanning microscopy images were recorded of human dermal microvascular endothelial cells (HDMEC) on a CPC scaffold incorporated with VEGF loaded or blank microparticles, which had been held in a humid atmosphere for 3 days. The images indicate that VEGF-loaded CPC scaffolds increased HDMEC cell proliferation and attachment on days 1 and 7 (Fig. 5C). In a similar study, Kim et al. demonstrated that bone morphogenetic protein-2–loaded nanoparticles with polycaprolactone (PCL-BMP-2/NPs) coating on a 3D printed hydroxyapatite (HAp) scaffold significantly increased human mesenchymal stem cell (hMSC) proliferation compared to the control (Fig. 5D) [146]. PCL-BMP2/NPs also increased the capacity for new bone formation after 8 weeks of implantation compared to the empty scaffold and 3D printed HAp (Fig. 5E).

### 6.2. Polymeric 3D printed biomaterials as drug delivery vehicles to treat bone disorders

Polymers have a long history in biomedical applications for orthopedic, dental, cardiovascular, and soft tissue constructs, and perhaps they are the most commonly utilized materials in bone tissue engineering applications as drug delivery vehicles [147]. Naturally sourced polymers such as collagen, fibrinogen, silk, chitosan, hyaluronate and alginate are used in orthopedic applications [148]. Although natural polymers have the potential advantage of biological recognition, which makes them biocompatible and biodegradable, they have several drawbacks, including immunogenicity, challenges in processing and reproducibility, and risk of transmitting pathogens from animals [149]. On the other hand, synthetic polymers provide great design flexibility and excellent control of mechanical and chemical properties, making them a more attractive choice for drug delivery vehicles in orthopedic applications. One of the disadvantages of using synthetic polymers is the risk of potential pH reduction in the localized area due to the hydrolytic degradation and formation of acidic by-products.

With the advent of 3D printing, synthetic polymers of α-hydroxy esters such as polygly*co*lic acid (PGA), polylactic acid (PLA), and a copolymer of these two monomers, polylactic-*co*-glycolic acid (PLGA), are often customized into 3D shapes with designed interconnected pores for drug delivery applications [150]. Apart from excellent biocompatibility, these polymers also exhibit non-enzymatic hydrolysis and generate non-toxic byproducts like carbon dioxide and water, which are easily eliminated from the body. Additional polymers being researched for bone tissue engineering applications include polycaprolactone (PCL), polyethylene glycol (PEG), polyanhydrides, polycarbonates, and polyfumarates [151–155]. PCL, owing to its impressive mechanical properties and desired biocompatibility, has been utilized to develop a sustained drug delivery carrier. *In vivo* and *in vitro* results have shown that 3D printed polymer scaffolds incorporated with therapeutic molecules enhance osteogenesis, as shown in Fig. 6. A recent study demonstrated potential of 3D printed PCL scaffolds loaded with deferoxamine (DFO) and carboxymethyl chitosan for improving bone regeneration in large segmental bone defects (Figs. 6A–D) [156]. Porous polycaprolactone (PCL) scaffolds were manufactured by FDM (Fig. 6A) and treated with an amine solution to impart a positive charge to the surface. Negatively charged chitosan was added on the aminated scaffold surface, followed by positive-charged DFO incorporation. The microstructures of the PCL scaffold, the intermediate aminated PCL scaffold (PCH),

and the carboxymethyl chitosan/deferoxamine loaded PCL scaffold (PCD) were examined by SEM (Fig. 6B). PCL scaffolds show fast release of DFO within 20 h which can promote effective coupling angiogenesis and osteogenesis in damaged bone. Results of micro-CT scans indicate that PCD shows the highest new bone formation and integration with the scaffold, followed by PCH, PCL, and CON (rats without scaffolds) (Fig. 6C). Hematoxylin and eosin (H&E) staining images indicated that PCD shows the highest new bone ingrowth and vascular formation compared to any other groups after four weeks of implantation (Fig. 6D). Lee et al. fabricated a 3D printed PCL scaffold (PCLS) with the 3D bio-printing system [157]. Recombinant human bone morphogenic protein-2 (rhBMP2) was incorporated with a polydopamine coating on PCLS to evaluate *in vitro* osteoconductivity (Fig. 6E). The rhBMP2 was incorporated by soaking a polydopamine-coated PCL scaffold in rhBMP2 solution (500 ng/ml and 10 mM Tris buffer, PCLSD 500) for 24 h at room temperature, and controlled rhBMP2 release was achieved in PBS (Fig. 6F). rhBMP2 released from dopamine-coated PCL (PCLSD) promotes cell growth and proliferation in MC3T3-E1 cells compared to the controls (PCLS and PCLSD) after day 7 (Fig. 6G).

Hydrophilic polymers such as PEG are widely used as drug delivery carriers, however, their poor mechanical properties limit these polymers to no- or low-load-bearing applications. Bone is a natural ceramic-polymer composite made of inorganic apatite reinforcements within the organic collagen matrix. Thus, ceramic-polymer composite materials are considered to be excellent choices as bone tissue engineering scaffolds. Numerous ceramic-polymer composite scaffolds such as PCL/HA, PLGA/HA, PLLA (Poly-L-lactic acid)/HA, PVA (polyvinyl alcohol)/HA, PP (polypropylene)/TCP have been investigated for drug delivery purposes [158–162]. These composites have shown significantly improved mechanical and biological properties compared to pure ceramic and polymer scaffolds.

### 6.3. Metallic 3D printed biomaterials as drug delivery vehicles to treat bone disorders

For over 100 years, metals and their alloys have been commonly used as load-bearing implant material for various dental and orthopedic applications due to their superior mechanical strength [163]. In the early 1900s, stainless steel (316 L steel or ASTM F138) and cobalt-based alloys (Co-Cr-Mo alloys, ASTM F75, F799) were primarily employed as the standards for making load-bearing prosthesis; these materials were landmarks for the development of modern metallic implants. Although these implants provided the desired mechanical strength, easy manufacturability, and good tolerance, they still had a higher modulus of elasticity and inferior biocompatibility compared to what was desired for biomedical materials. Nonetheless, titanium (Ti) soon became the material of choice for orthopedic implantable devices due to its lower elastic modulus, excellent tissue compatibility, higher corrosion resistance, and superior specific strength. Although commercially pure titanium (ASTM F67) demonstrated excellent osseointegration due to the oxide layer surface, its alloy Ti6Al4V ELI (ASTM F136) gained more popularity in subsequent years for its ultra-low elastic modulus (110 GPa), less than half that of 316 stainless steels [164].

Recent developments in materials chemistry, manufacturing, and metallurgy continue to spur innovations in designs and diversifications of metal implants. However, metal-based

drug delivery implants have received limited attention compared to polymer or ceramic-based carriers, despite their unique advantages in localized drug delivery. Part of the reason for their limited application as drug-eluting carriers is their lack of biological interaction on the surface of the material, which causes poor tissue-material interactions. Another disadvantage of metallic biomaterials is the release of toxic metal ions and particulate debris through *in vivo* corrosion or wear, which can lead to adverse biological reactions and tissue damage [15]. Numerous surface coating and modification strategies have been developed to overcome these challenges to improve tissue-implant interaction and subsequent osseointegration, preserving the inherent mechanical properties of metallic biomaterials [165].

Several studies have shown metallic implants coated with hydrophobic or hydrophilic biodegradable polymer matrices can be used as controllable means to deliver drugs *via* diffusion mechanisms. Ceramic coatings such as hydroxyapatite soon became some of the most common coating techniques for localized drug delivery in orthopedic applications and gained more popularity than polymers due to their excellent bioactivity and compositional similarity to bone [166,167]. Considerable research has focused on the prevention and treatment of implant-related infection (IRI) by incorporating antibiotics within polymer and ceramic matrices, which release antibiotics in a sustained manner, limiting local toxicity from high concentrations of antibiotics [168–171]. *In vivo* and *in vitro* results have shown that ceramic-coated 3D printed metal scaffolds incorporated with therapeutic compounds promote osteogenesis, angiogenesis, and antibacterial properties, as shown in Fig. 7. One study investigated the osteogenic and angiogenic responses to vascular endothelial growth factor (VEGF) loaded silicon substituted hydroxyapatite (SiHA) coated Ti6Al4V scaffold *in vitro* and *in vivo* [172]. The porous Ti6Al4V scaffolds were manufactured using electron-beam melting (EBM); VEGF was loaded onto the Ti6Al4V scaffolds after they had been coated with SiHA (Fig. 7A and B). The presence of VEGF enhanced cell viability and the proliferation of pre-osteoblastic cells as well as EC2 mature endothelial cells after 3 days of incubation. Optical microscopy images of histological sections after Masson-Goldner's trichrome staining and von Kossa's staining demonstrated that the release of VEGF from the implant enhanced trabeculae development and angiogenesis in the *in vivo* sheep model (Fig. 7C and D). Another study showed that 3D printed stainless steel scaffolds achieved biocompatibility and antibacterial properties when covered with a Ag incorporated zeolite coating [173]. Selective laser melting (SLA) was used to create a microporous structure of 316 L stainless steels (316 L SS, Control). To evaluate the antibacterial efficacy of silver release from 316 L SS, a zeolite film (ZCs) and Ag-incorporated ZCs (Ag-ZCs) were utilized to coat the 316 L SS. The SEM images indicate that the 316 L SS has interconnected macro pores of 800 μm (Fig. 7E). No morphological changes were observed after applying the zeolite film with Ag incorporation. A zone of inhibition assay showed that Ag-ZCs inhibit the growth of *S.aureus* and *E. coli* compared with other groups (Control and ZCs) after 24 h (Fig. 7F). SEM images of *S.aureus* and *E. coli* on samples after 24 h demonstrate that the number of colonies of these bacteria on Ag-ZCs is much lower than on the control and ZCs. None of the scaffolds were cytotoxic to bone marrow stromal cells (BMSCs) at day 5 (Fig. 7G).

The inherent porous structure of the hydroxyapatite matrix acts as a unique drug reservoir, which allows optimum loading and controlled release of therapeutic agents. Ti naturally forms an oxide layer on its surface and anodization can further be utilized to synthesize nanotubes on the metal surface. Titania nanotube arrays show potential as a promising drug delivery system due to their excellent biocompatibility, high surface area, desired bioactivity, and capability to load and release drugs *in vivo*. The titania nanotubes have a porous nanotubular structure, which enables them to be loaded with antimicrobial therapeutic agents [174].

Other than coating techniques, researchers have also attempted to covalently attach antibiotics to the implant surface to prevent the adherence of bacteria and implant-related bacterial infections. Although not utilized frequently, other drug delivery carriers, such as self-assembled monolayers and porous metal structures, were also explored in conjunction with Ti for their drug-eluting capabilities. A few studies have explored the potential for controlled antibiotic delivery *via* self-assembling antimicrobial peptides, biodegradable magnesium foam, and non-degradable porous stainless steel implants [175–179]. Table 5 lists different 3D printed polymeric, ceramic, and metallic bone substitutes, their manufacturing processes, and their ability to deliver biomolecules to treat major orthopedic and dental complications.

### 6.4. Natural medicine delivery from 3D printed biomaterials as drug delivery vehicles to treat bone disorders

The integration of pharmaceutical compounds and growth factors with 3D printed scaffolds has been extensively utilized in bone tissue engineering. Nevertheless, these methodologies frequently restrict clinical implementations due to drug resistance, exorbitant expenses, and cytotoxicity concerns. NMCs are natural therapeutic alternatives with demonstrated effectiveness in the management of diverse bone pathologies. However, the limited bioavailability of these compounds has hindered their clinical translations. The nonpolar/hydrophobic properties of NMCs also limit their use in systems designed for controlled release. Recent studies have addressed these limitations by introducing various types of polymer coatings and novel drug delivery carriers. In a recent study, the incorporation of *Cissus quadrangularis* extract (CQE) with 3D printed TCP scaffolds was introduced using a polydopamine coating (Fig. 8A–C) [121]. The polydopamine coating increased the release rate of CQE from the scaffolds without compromising their mechanical strength; the coating also enhanced biological properties both *in vitro* and *in vivo*. The results of an ALP assay indicated that *in vitro* differentiation of osteoblast cells was enhanced by the polydopamine coating with 200 μg of CQE ($CQE_L$) when compared to the control group (Fig. 8B). Masson Goldner staining images revealed that the presence of CQE combined with the polydopamine coating on 3D printed scaffolds improved new bone formation (Fig. 8C). Another *in vitro* study found that a controlled release of soy isoflavones occurs as a result of hydrophobic interactions and competitive electrostatic interactions between soy isoflavones, scaffold degradation, drug solubility changes, and drug-protein complex formation [18]. Soy isoflavones released from 3D printed scaffolds increased osteoblast cell proliferation and cell attachment in a bioreactor system after 5 days (Fig. 8E), and also improved *in vitro* osteoblast cell differentiation at day 10 in the bioreactor system, as compared to the control

(Fig. 8F). Similarly, gingerol and allicin were loaded into a 3D printed TCP scaffold with a PCL/PEG coating to increase the rate of gingerol and allicin release (Fig. 8G) and to evaluate their biological properties *in vivo* [122]. H&E staining revealed that gingerol and allicin in combination with PCL/PEG (T + G + A + PP) increase osteocytes and new bone area by 90% and 30%, respectively, compared to the control tricalcium phosphate scaffold (Fig. 8H). Optical micrographs of modified Masson-Goldner trichrome stained sections demonstrate that bone mineralization in the presence of gingerol and gingerol+allicin (gingerol and allicin) was increased at week 10 compared to control TCP (Fig. 8I). NMCs incorporated within 3D printed scaffolds also showed anti-inflammatory and anti-cancer properties. The anti-inflammatory effects of soy isoflavone loaded 3D printed TCP scaffolds were evaluated using the *in vivo* animal model [18]. Optical microscopy images of hematoxylin and eosin (H&E) staining 24 h after implementation showed inflammatory cells in all samples (Fig. 9A). However, measurement of neutrophil recruitment based on H&E staining indicates that genistein and a combination of genistein, daidzein, and glycitein in a 5:4:1 ratio reduced neutrophil recruitment compared to the control. In another study, liposomal curcumin was incorporated within 3D printed calcium phosphate scaffolds to control the rate of curcumin release and enhance the *in vitro* biological properties of the curcumin (Fig. 9B) [81]. This study demonstrated that liposome-encapsulated curcumin exhibited sustained release from the bone scaffold, which in turn improved *in vitro* osteoblast proliferation and chemoprevention compared to the free curcumin loaded bone scaffolds (Fig. 9C). In yet another study, pH responsive epigallocatechin gallate (EGCG) release from a 3D printed TCP scaffold enhanced the biological properties of the scaffolds for bone tissue engineering [191], thereby improving *in vitro* osteoblast cell proliferation and cell attachment on the scaffolds (Fig. 9D). The *in vitro* osteogenic potential of EGCG is realized by upregulating osteoblast differentiation marker expressions such as Runt-related transcription factor 2 (Runx2) and bone gamma-carboxyglutamic acid-containing protein (BGLAP). EGCG release also induced endothelial tube formation, revealing its *in vitro* angiogenesis activities. However, EGCG loaded 3D printed scaffolds inhibited *in vitro* osteosarcoma proliferation (Fig. 9E). Clearly, the incorporation of NMCs in 3D printed scaffolds demonstrated tremendous capability in treating bone disorders, as summarized in Table 5.

## 7. Critical concerns related to natural medicinal compounds

### 7.1. Batch to batch variation and isolation

The primary active components of medicinal plants and their concentrations vary depending on the geographic origin and growing conditions, including temperature, humidity, harvest time, storage conditions, and seasonal variation. In addition, herbal plants have a complex mixture of more than one active ingredient with multiple potential targets. Often, active compounds are isolated and identified after purification with advanced technologies such as liquid chromatography, nuclear magnetic resonance (LC-NMR) and liquid chromatography-mass spectrometry (LC-MS). However, such approaches require reference standard compounds to identify the medicinal compounds. Proper knowledge of extraction and separation techniques for NMCs is crucial since the techniques vary from species to species. The purification process enhances the pharmaceutical efficacy of herbal

medicine by removing impurities and helps determine the chemical profiles used to predict drug properties.

### 7.2. Dosage and toxicity

Medicinal plants are prone to accumulating heavy metals from contaminated soil and such contamination can pose a serious risk for poisoning. This type of bioaccumulation in medicinal plants varies depending on the parts of the plant used and the geographical regions and weather patterns where the plant was cultivated [194]. Detoxification procedures are usually carried out to remove toxic or undesired parts from the herbal plant through a series of processing steps, including pre-treatment methods such as physical processing, chemical modification, and purification. Physical processing including cleaning, cutting, and steaming reduces toxicity and enhances pharmaceutical efficacy [195]. Structural or chemical modifications of the extracts are also carried out to minimize toxicity and increase pharmacological efficacy [196]. (5*R*)-5-hydroxytriptolide (LLDT-8) is a medicinal compound (isolated from *Tripterygium* using high-performance liquid chromatography) that has shown efficacy and safety in the application of artificial grafts [197]. Since chemical modification can alter pharmaceutical efficacy and safety, it requires careful consideration for pharmaceutical applications. Lastly, purification of natural compounds is a crucial step that removes contaminants from plant products, thereby avoiding the occurrence of adverse effects while enhancing pharmaceutical efficacy.

### 7.3. Standardization of natural medicinal compounds

The appropriate dosages and toxicity levels of each NMC along with quality control have been identified as the most crucial monitoring parameters to ensure the safety and efficacy of NMCs. However, the safety standards of NMCs fail to meet basic requirements as the recommended dosages vary depending on the recommending organizations, including the World Health Organization (WHO) and others [198]. The Federal Drug Administration (FDA) in the United States also has established guidelines for the marketing and sale of herbal medicines [199]. Due to the lack of standardization, inappropriate or high dosages of natural medications are quite common and pose a real risk to public health and safety. Apart from the issue of standardization, transparent information about cultivation conditions and toxicity test results will be useful for determining appropriate dosage levels for patients. Clinical and pre-clinical trials using NMCs will guide the optimization of dosage standardization, determine toxicity levels, and expand the knowledge of herbal medicine regarding drug mechanisms and interactions.

## 8. Summary and future perspectives

3D printing technologies have enabled the development of patient-specific implants by modulating the internal architecture of the implant to mimic the physical characteristics of human bone tissue. Various biocompatible materials including metals, ceramics, polymers, and composites are available for the fabrication of implants using 3D printing technology; material selection depends on the location of the bone defect site and the type of bone loss.

Tremendous advances have been made in implant materials and technologies. The FDA has issued a guidebook for 3D printed medical implants titled “Technical Considerations for Additive Manufactured Medical Devices” [200]. Using these guidelines, the enhanced multifunctional bone implants should balance innovation and safety to deliver patient satisfaction and positive treatment outcomes. The FDA has implemented an approval process for new implant designs and components to ensure the safe and effective use of bone implants. The FDA also inspects medical devices for compliance with regulations that govern layout, components, printing methods, sterilization, physical and mechanical tests, quality checks, printing parameters, and biocompatibility [201,202].

Despite recent advances, implants do not always restore the biological function of native bone tissue. Active pharmaceutical ingredients can be integrated into the implants and can be used to overcome the limitations of conventional implants for treating bone diseases and post-implantation pathologies. NMCs are promising candidates because of their unique physiological complexity, therapeutic simplicity, and wide range of biological effects [203–205]. However, several concerns need to be addressed for the effective implementation of NMCs for treating bone disorders: (1) batch-to-batch variation and reproducibility, (2) establishment of proper dosage, (3) purity and any possible unknown toxicity, (4) lack of standardization. Improvement in extraction and purification techniques will reduce the differences between NMC batches by eliminating impurities and isolating the desired active compound. In addition, NMC-based clinical and pre-clinical trials will suggest optimized dosages, confirm toxicity ranges, and expand herbal medicine knowledge regarding pharmacological mechanisms and interactions. Therefore, developing novel drug delivery systems requires a deeper understanding of connections between 3D printed bone implants and NMCs, along with process optimization and drug loading strategies.

3D printing technologies allow the modulation of implant structures that directly affect drug loading and controlled release. Modification of biomaterial chemistry also enables the incorporation of NMCs within 3D printed implants *via* physical and chemical interactions that improve cellular interactions and bone regeneration in critical-sized bone defects. Therefore, optimization of drug loading mechanism, drug delivery vehicles, structural parameters of the implants, surface modification of the implants, and the modulation of the drug release profile must be critically assessed while designing multifunctional 3D printed bone implants that incorporate NMCs. In other words, it is important to understand the structure-process-property relationships of these 3D printed systems for their use in effective on-site drug delivery. Further advancements can potentially satisfy critical clinical needs, especially for common musculoskeletal disorders and traumas, including osteoporosis, osteomyelitis, and osteoarthritis. Improved multifunctional 3D printed implants will continue to provide innovative clinical solutions for the secondary reconstruction of patient-specific bone defects and traumas with natural medicine.

## Acknowledgments

The authors would like to acknowledge financial support from the National Institute of Dental and Craniofacial Research (NIDCR) of the NIH grant number R01 DE029204–01 (PI: Bose) and the National Institute of Arthritis and Musculoskeletal and Skin Diseases (NIAMS) of the National Institutes of Health, USA under Award Number R56 AR066361 (PI: Bose).

## Data availability

Data will be made available on request.

## References


[1]. Office of the Surgeon General (US), Bone health and osteoporosis: a report of the Surgeon General, US Heal, Hum. Serv. (2004) 437.

[2]. Bonewald L, Use it or lose it to age: a review of bone and muscle communication, Bone. 120 (2019) 212–218, 10.1016/j.bone.2018.11.002. [PubMed: 30408611]

[3]. Burr DB, Changes in bone matrix properties with aging, Bone. 120 (2019) 85–93, 10.1016/j.bone.2018.10.010. [PubMed: 30315999]

[4]. Duda GN, Geissler S, Checa S, Tsitsilonis S, Petersen A, Schmidt-Bleek K, The decisive early phase of bone regeneration, Nat. Rev. Rheumatol. 19 (2023) 78–95, 10.1038/s41584-022-00887-0. [PubMed: 36624263]

[5]. Schmidt AH, Autologous bone graft: Is it still the gold standard? Injury. 52 (2021) S18–S22, 10.1016/J.INJURY.2021.01.043.

[6]. Hall BM, Cells Mediating Allograft Rejection, Transplantation 51, 1991. https://journals.lww.com/transplantjournal/Fulltext/1991/06000/CELLS_MEDIATING_ALLOGRAFT_REJECTION.1.aspx.

[7]. Betz RR, Limitations of autograft and allograft: New synthetic solutions, Orthopedics. 25 (2002), 10.3928/0147-7447-20020502-04.

[8]. Bose S, Roy M, Bandyopadhyay A, Recent advances in bone tissue engineering scaffolds, Trends Biotechnol. 30 (2012) 546–554, 10.1016/j.tibtech.2012.07.005. [PubMed: 22939815]

[9]. Bose S, Ke D, Sahasrabudhe H, Bandyopadhyay A, Additive manufacturing of biomaterials, Prog. Mater. Sci. 93 (2018) 45–111, 10.1016/j.pmatsci.2017.08.003. [PubMed: 31406390]

[10]. Bose S, Traxel KD, Vu AA, Bandyopadhyay A, Clinical significance of three-dimensional printed biomaterials and biomedical devices, MRS Bull. 44 (2019) 494–504, 10.1557/mrs.2019.121. [PubMed: 31371848]

[11]. Tofail SAM, Koumoulos EP, Bandyopadhyay A, Bose S, O'Donoghue L, Charitidis C, Additive manufacturing: scientific and technological challenges, market uptake and opportunities, Mater. Today 21 (2018) 22–37, 10.1016/j.mattod.2017.07.001.

[12]. Bose S, Sarkar N, Banerjee D, Natural medicine delivery from biomedical devices for the treatment of bone disorders: a review, Acta Biomater. 126 (2021) 63–91, 10.1016/j.actbio.2021.02.034. [PubMed: 33657451]

[13]. Bose S, Tarafder S, Calcium phosphate ceramic systems in growth factor and drug delivery for bone tissue engineering: a review, Acta Biomater. 8 (2012) 1401–1421, 10.1016/j.actbio.2011.11.017. [PubMed: 22127225]

[14]. Wani TU, Khan RS, Rather AH, Beigh MA, Sheikh FA, Local dual delivery therapeutic strategies: using biomaterials for advanced bone tissue regeneration, J. Control. Release 339 (2021) 143–155, 10.1016/j.jconrel.2021.09.029. [PubMed: 34563589]

[15]. Bose S, Robertson SF, Bandyopadhyay A, Surface modification of biomaterials and biomedical devices using additive manufacturing, Acta Biomater. 66 (2018) 6–22, 10.1016/j.actbio.2017.11.003. [PubMed: 29109027]

[16]. Yang YP, Labus KM, Gadomski BC, Bruyas A, Easley J, Nelson B, Palmer RH, McGilvray K, Regan D, Puttlitz CM, Stahl A, Lui E, Li J, Moeinzadeh S, Kim S, Maloney W, Gardner MJ, Osteoinductive 3D printed scaffold healed 5 cm segmental bone defects in the ovine metatarsus, Sci. Rep. 11 (2021) 1–12, 10.1038/s41598-021-86210-5. [PubMed: 33414495]

[17]. Vu AA, Bose S, Natural antibiotic Oregano in hydroxyapatite-coated titanium reduces osteoclastic bone resorption for orthopedic and dental applications, ACS Appl. Mater. Interfaces 12 (2020) 52383–52392, 10.1021/acsami.0c14993. [PubMed: 33181015]

[18]. Sarkar N, Bose S, Controlled release of soy isoflavones from multifunctional 3D printed bone tissue engineering scaffolds, Acta Biomater. 114 (2020) 407–420, 10.1016/j.actbio.2020.07.006. [PubMed: 32652224]

[19]. Bose S, Bhattacharjee A, Huynh C, Banerjee D, Allicin-loaded hydroxyapatite: enhanced release, cytocompatibility, and antibacterial properties for bone tissue engineering applications, JOM. 74 (2022) 3349–3356, 10.1007/s11837-022-05366-1. [PubMed: 36568491]

[20]. Sarkar N, Morton H, Bose S, Effects of vitamin C on osteoblast proliferation and osteosarcoma inhibition using plasma coated hydroxyapatite on titanium implants, Surf. Coat. Technol. 394 (2020), 125793, 10.1016/j.surfcoat.2020.125793. [PubMed: 32612317]

[21]. Sarkar N, Bose S, Controlled delivery of curcumin and vitamin K2 from hydroxyapatite-coated titanium implant for enhanced *in Vitro* Chemoprevention, Osteogenesis, and *in Vivo* Osseointegration, ACS Appl. Mater. Interfaces 12 (2020) 13644–13656, 10.1021/acsami.9b22474. [PubMed: 32013377]

[22]. Banerjee D, Bose S, Effects of aloe vera gel extract in doped hydroxyapatite-coated titanium implants on in vivo and in vitro biological properties, ACS Appl. Bio Mater. 2 (2019) 3194–3202, 10.1021/acsabm.9b00077.

[23]. Ghahfarrokhi SH, Reisi R, Effects of medicinal herbs on osteoporosis: a systematic review based on clinical trials, Shahrekord Univ. Med. Sci. 21 (2019) 229–236, 10.34172/jsums.2019.40.

[24]. Potu BK, Rao MS, Nampurath GK, Chamallamudi MR, Prasad K, Nayak SR, Dharmavarapu PK, Kedage V, Bhat KMR, Evidence-based assessment of antiosteoporotic activity of petroleum-ether extract of *Cissus quadrangularis* Linn. on ovariectomy-induced osteoporosis, Ups, J. Med. Sci. 114 (2009) 140–148, 10.1080/03009730902891784. [PubMed: 19736603]

[25]. Wang QL, Huo XC, Wang JH, Wang DP, Zhu QL, Liu B, Xu LL, Rutin prevents the ovariectomy-induced osteoporosis in rats, Eur. Rev. Med. Pharmacol. Sci. 21 (2017) 1911–1917. [PubMed: 28485786]

[26]. Nowak B, Matuszewska A, Nikodem A, Filipiak J, Landwójtowicz M, Sadanowicz E, Jędrzejuk D, Rzeszutko M, Zduniak K, Piasecki T, Kowalski P, Dziewiszek W, Merwid-Ląd A, Trocha M, Sozański T, Kwiatkowska J, Bolanowski M, Szeląg A, Oral administration of kaempferol inhibits bone loss in rat model of ovariectomy-induced osteopenia, Pharmacol. Rep. 69 (2017) 1113–1119, 10.1016/j.pharep.2017.05.002. [PubMed: 29031689]

[27]. Sun X, Li F, Ma X, Ma J, Zhao B, Zhang Y, Li Y, Lv J, Meng X, The effects of combined treatment with Naringin and treadmill exercise on Osteoporosis in Ovariectomized rats, Sci. Rep. 5 (2015) 1–9, 10.1038/srep13009.

[28]. Hohman EE, Weaver CM, A grape-enriched diet increases bone calcium retention and cortical bone properties in ovariectomized rats, J. Nutr. 145 (2015) 253–259, 10.3945/jn.114.198598. [PubMed: 25644345]

[29]. Wu Y, Cao L, Xia L, Wu Q, Wang J, Wang X, Xu L, Zhou Y, Xu Y, Jiang X, Evaluation of Osteogenesis and angiogenesis of Icariin in local controlled release and systemic delivery for calvarial defect in Ovariectomized rats, Sci. Rep. 7 (2017) 1–14, 10.1038/s41598-017-05392-z. [PubMed: 28127051]

[30]. Huang Q, Gao B, Jie Q, Wei BY, Fan J, Zhang HY, Zhang JK, Li XJ, Shi J, Luo ZJ, Yang L, Liu J, Ginsenoside-Rb2 displays anti-osteoporosis effects through reducing oxidative damage and bone-resorbing cytokines during osteogenesis, Bone. 66 (2014) 306–314, 10.1016/j.bone.2014.06.010. [PubMed: 24933344]

[31]. Tande AJ, Patel R, Prosthetic joint infection, Clin. Microbiol. Rev. 27 (2014) 302–345, 10.1128/CMR.00111-13. [PubMed: 24696437]

[32]. Hatzenbuehler J, Pulling TJ, Diagnosis and management of Osteomyelitis, Am. Fam. Physician 84 (2011) 1027–1033. [PubMed: 22046943]

[33]. Arciola CR, An YH, Campoccia D, Donati ME, Montanaro L, Etiology of implant orthopedic infections: a survey on 1027 clinical isolates, Int. J. Artif. Organs. 28 (2005) 1091–1100, 10.1177/039139880502801106. [PubMed: 16353115]

[34]. Lew DP, Waldvogel FA, Osteomyelitis, Lancet (British Ed) 364 (2004) 369–379, 10.1016/S0140-6736(04)16727-5.

[35]. Mistry S, Roy R, Jha AK, Pandit N, Das S, Burman S, Joy M, Treatment of long bone infection by a biodegradable bone cement releasing antibiotics in human, J. Control. Release 346 (2022) 180–192, 10.1016/j.jconrel.2022.04.018. [PubMed: 35447299]

[36]. Silva LN, Zimmer KR, Macedo AJ, Trentin DS, Plant natural products targeting bacterial virulence factors, Chem. Rev. 116 (2016) 9162–9236, 10.1021/acs.chemrev.6b00184. [PubMed: 27437994]

[37]. Hultgren SJ, Cegelski L, Marshall GR, Eldridge GR, The biology and future prospects of antivirulence therapies, Nat. Rev. Microbiol. 6 (2008) 17–27, 10.1038/nrmicro1818. [PubMed: 18079741]

[38]. Newman DJ, Cragg GM, Natural products as sources of new drugs over the nearly four decades from 01/1981 to 09/2019, J. Nat. Prod. 83 (2020) 770–803, 10.1021/acs.jnatprod.9b01285. [PubMed: 32162523]

[39]. Zhai H, Pan J, Pang E, Bai B, Lavage with allicin in combination with vancomycin inhibits biofilm formation by *Staphylococcus epidermidis* in a rabbit model of prosthetic joint infection, PLoS One 9 (2014), 10.1371/journal.pone.0102760.

[40]. Lu M, Dai T, Murray CK, Wu MX, Bactericidal property of oregano oil against multidrug-resistant clinical isolates, Front. Microbiol. 9 (2018) 1–14, 10.3389/fmicb.2018.02329. [PubMed: 29403456]

[41]. Zhou Z, Pan C, Lu Y, Gao Y, Liu W, Yin P, Yu X, Combination of erythromycin and curcumin alleviates *Staphylococcus aureus* induced osteomyelitis in rats, Front. Cell. Infect. Microbiol. 7 (2017) 1–6, 10.3389/fcimb.2017.00379. [PubMed: 28149830]

[42]. Zhou W, Wang Z, Mo H, Zhao Y, Li H, Zhang H, Hu L, Zhou X, Thymol mediates bactericidal activity against *staphylococcus aureus* by targeting an aldo-keto reductase and consequent depletion of NADPH, J. Agric. Food Chem. 67 (2019) 8382–8392, 10.1021/acs.jafc.9b03517. [PubMed: 31271032]

[43]. Dusane DH, Kyrouac D, Petersen I, Bushrow L, Calhoun JH, Granger JF, Phieffer LS, Stoodley P, Targeting intracellular *Staphylococcus aureus* to lower recurrence of orthopedic infection, J. Orthop. Res. 36 (2018) 1086–1092, 10.1002/jor.23723. [PubMed: 28885721]

[44]. Rampogu S, Baek A, Gajula RG, Zeb A, Bavi RS, Kumar R, Kim Y, Kwon YJ, Lee KW, Ginger (Zingiber officinale) phytochemicals-gingerenone-A and shogaol inhibit SaHPPK: Molecular docking, molecular dynamics simulations and *in vitro* approaches, Ann. Clin. Microbiol. Antimicrob. 17 (2018) 1–15, 10.1186/s12941-018-0266-9. [PubMed: 29391040]

[45]. Salah F, El Ghoul Y, Mahdhi A, Majdoub H, Jarroux N, Sakli F, Effect of the deacetylation degree on the antibacterial and antibiofilm activity of acemannan from Aloe vera, Ind. Crop. Prod. 103 (2017) 13–18, 10.1016/j.indcrop.2017.03.031.

[46]. Mirabello L, Troisi RJ, Savage SA, Osteosarcoma incidence and survival rates from 1973 to 2004: data from the surveillance, epidemiology, and end results program, Cancer. 115 (2009) 1531–1543, 10.1002/cncr.24121. [PubMed: 19197972]

[47]. Durfee RA, Mohammed M, Luu HH, Review of Osteosarcoma and current management, Rheumatol. Ther. 3 (2016) 221–243, 10.1007/s40744-016-0046-y. [PubMed: 27761754]

[48]. Misaghi A, Goldin A, Awad M, Kulidjian AA, Osteosarcoma: a comprehensive review, Sicot-J. 4 (2018) 12, 10.1051/sicotj/2017028. [PubMed: 29629690]

[49]. Ferrari S, Serra M, An update on chemotherapy for osteosarcoma, Expert. Opin. Pharmacother. 16 (2015) 2727–2736, 10.1517/14656566.2015.1102226. [PubMed: 26512909]

[50]. Eilber F, Giuliano A, Eckardt J, Patterson K, Moseley S, Goodnight J, Adjuvant chemotherapy for osteosarcoma: a randomized prospective trial, J. Clin. Oncol. 5 (1987) 21–26, 10.1200/JCO.1987.5.1.21. [PubMed: 3543236]

[51]. Faisham WI, Mat Saad AZ, Alsaigh LN, Nor Azman MZ, Kamarul Imran M, Biswal BM, Bhavaraju VMK, Salzihan MS, Hasnan J, Ezane AM, Ariffin N, Norsarwany M, Ziyadi MG, Wan Azman WS, Halim AS, Zulmi W, Prognostic factors and survival rate of osteosarcoma: a single-institution study, Asia, Pac. J. Clin. Oncol. 13 (2017) e104–e110, 10.1111/ajco.12346.

[52]. Abe K, Maeda-Minami A, Ishizu T, Iwata S, Kobayashi E, Shimoi T, Kawano Y, Hashimoto H, Yamaguchi M, Furukawa T, Miyazaki S, Mano Y, Risk factors for hepatic toxicity of high-dose

methotrexate in patients with Osteosarcoma, Anticancer Res. 42 (2022) 1043–1050, 10.21873/anticanres.15565. [PubMed: 35093905]

[53]. van Dalen EC, van der Pal HJH, Caron HN, Kremer LCM, Different dosage schedules for reducing cardiotoxicity in cancer patients receiving anthracycline chemotherapy, Cochrane Database Syst. Rev. (2006) CD005008. [PubMed: 17054232]

[54]. Huang M, Lu JJ, Ding J, Natural products in cancer therapy: past, present and future, Nat. Prod. Bioprospect. 11 (2021) 5–13, 10.1007/s13659-020-00293-7. [PubMed: 33389713]

[55]. Roy A, Datta S, Bhatia KS, Bhumika P, Prasad Jha R, Role of plant derived bioactive compounds against cancer, South African J. Bot. 149 (2021) 1017–1028, 10.1016/j.sajb.2021.10.015.

[56]. Taylor WF, Yanez M, Moghadam SE, Farimani MM, Soroury S, Ebrahimi SN, Tabefam M, Jabbarzadeh E, 7-Epi-clusianone, a multi-targeting natural product with potential chemotherapeutic, immune-modulating, and anti-angiogenic properties, Molecules. 24 (2019), 10.3390/molecules24234415.

[57]. Chang R, Sun L, Webster TJ, Short communication: selective cytotoxicity of curcumin on osteosarcoma cells compared to healthy osteoblasts, Int. J. Nanomedicine 9 (2014) 461–465, 10.2147/IJN.S55505. [PubMed: 24453488]

[58]. Zhu K, Wang W, Green tea polyphenol EGCG suppresses osteosarcoma cell growth through upregulating miR-1, Tumor Biol. 37 (2016) 4373–4382, 10.1007/s13277-015-4187-3.

[59]. Li Z, Ding X, Wu H, Liu C, Artemisinin inhibits angiogenesis by regulating p38 MAPK/CREB/TSP-1 signaling pathway in osteosarcoma, J. Cell. Biochem. 120 (2019) 11462–11470, 10.1002/jcb.28424. [PubMed: 30746754]

[60]. Jin H, Jin X, Cao B, Wenbo W, Berberine affects osteosarcoma *via* downregulating the caspase-1/IL-1β signaling axis, Oncol. Rep. 37 (2017) 729–736, 10.3892/OR.2016.5327. [PubMed: 28000894]

[61]. Li X-F, Zhao G-Q, Li L-Y, Ginsenoside impedes proliferation and induces apoptosis of human osteosarcoma cells by down-regulating beta-catenin, Cancer Biomark. 24 (2019) 395–404, 10.3233/CBM-182046. [PubMed: 30909183]

[62]. Lin CC, Kuo CL, Lee MH, Lai KC, Lin JP, Yang JS, Yu CS, Lu CC, Chiang JH, Chueh FS, Chung JG, Wogonin triggers apoptosis in human osteosarcoma U-2 OS cells through the endoplasmic reticulum stress, mitochondrial dysfunction and caspase-3-dependent signaling pathways, Int. J. Oncol. 39 (2011) 217–224, 10.3892/ijo.2011.1027. [PubMed: 21573491]

[63]. Ying J, Xu H, Wu D, Wu X, Emodin induces apoptosis of human osteosarcoma cells via mitochondria- and endoplasmic reticulum stress-related pathways, Int. J. Clin. Exp. Pathol. 8 (2015) 12837–12844. [PubMed: 26722474]

[64]. Hsieh YS, Chu SC, Yang SF, Chen PN, Liu YC, Lu KH, Silibinin suppresses human osteosarcoma MG-63 cell invasion by inhibiting the ERK-dependent c-Jun/AP-1 induction of MMP-2, Carcinogenesis. 28 (2007) 977–987, 10.1093/carcin/bgl221. [PubMed: 17116726]

[65]. Huang T, Zhang X, Wang H, Punicalagin inhibited proliferation, invasion and angiogenesis of osteosarcoma through suppression of NF-κB signaling, Mol. Med. Rep. 22 (2020) 2386–2394, 10.3892/mmr.2020.11304. [PubMed: 32705250]

[66]. Glyn-Jones S, Palmer AJR, Agricola R, Price AJ, Vincent TL, Weinans H, Carr AJ, Osteoarthritis, Lancet (British Ed) 386 (2015) 376–387, 10.1016/S0140-6736(14)60802-3.

[67]. Primorac D, Molnar V, Rod E, Jeleč Ž, Čukelj F, Matišić V, Vrdoljak T, Hudetz D, Hajsok H, Borić I, Knee osteoarthritis: a review of pathogenesis and state-of-the-art non-operative therapeutic considerations, Genes (Basel) 11 (2020) 1–35, 10.3390/genes11080854.

[68]. Nelson AE, Allen KD, Golightly YM, Goode AP, Jordan JM, A systematic review of recommendations and guidelines for the management of osteoarthritis: the Chronic Osteoarthritis Management Initiative of the U.S. Bone and joint initiative, semin, Arthritis Rheum. 43 (2014) 701–712, 10.1016/j.semarthrit.2013.11.012.

[69]. Majeed MH, Sherazi SAA, Bacon D, Bajwa ZH, Pharmacological treatment of pain in Osteoarthritis: a descriptive review, Curr. Rheumatol. Rep. 20 (2018) 1–10, 10.1007/s11926-018-0794-5.

[70]. McCarthy GM, McCarty DJ, Effect of topical capsaicin in the therapy of painful osteoarthritis of the hands, J. Rheumatol. 19 (1992) 604–607, http://europepmc.org/abstract/MED/1375648. [PubMed: 1375648]

[71]. Persson MSM, Stocks J, Walsh DA, Doherty M, Zhang W, The relative efficacy of topical non-steroidal anti-inflammatory drugs and capsaicin in osteoarthritis: a network meta-analysis of randomized controlled trials, Osteoarthr. Cartil. 26 (2018) 1575–1582, 10.1016/j.joca.2018.08.008.

[72]. Shah BN, Seth AK, Maheshwari KM, A review on medicinal plants as a source of anti-inflammatory agents, Res. J. Med. Plant. 5 (2011) 101–115, 10.3923/rjmp.2011.101.115.

[73]. Reis Nunes C, Barreto Arantes M, Menezes de Faria Pereira S, Leandro da Cruz L, De Souza Passos M, Pereira de Moraes L, Curcino Vieira IJ, Barros de Oliveira D, Plants as sources of anti-inflammatory agents, Molecules. 25 (2020) 1–22.

[74]. Persson MSM, Stocks J, Walsh DA, Doherty M, Zhang W, The relative efficacy of topical non-steroidal anti-inflammatory drugs and capsaicin in osteoarthritis: a network meta-analysis of randomized controlled trials, Osteoarthr. Cartil. 26 (2018) 1575–1582, 10.1016/j.joca.2018.08.008.

[75]. Altman RD, Marcussen KC, Effects of a ginger extract on knee pain in patients with osteoarthritis, Arthritis Rheum. 44 (2001) 2531–2538, 10.1002/1529-0131(200111)44:11 < 2531::AID-ART433 > 3.0.CO;2-J. [PubMed: 11710709]

[76]. Gao F, Zhang S, Salicin inhirits AGE-induced degradation of type II collagen and aggrecan in human SW1353 chondrocytes: therapeutic potential in osteoarthritis, Artif. Cells Nanomed. Biotechnol. 47 (2019) 1043–1049, 10.1080/21691401.2019.1591427. [PubMed: 30942091]

[77]. Shep D, Khanwelkar C, Gade P, Karad S, Safety and efficacy of curcumin versus diclofenac in knee osteoarthritis: a randomized open-label parallel-arm study, Trials. 20 (2019) 1–11, 10.1186/s13063-019-3327-2. [PubMed: 30606236]

[78]. Ho LJ, Hung LF, Liu FC, Hou TY, Lin LC, Huang CY, Lai JH, *Ginkgo biloba* extract individually inhibits JNK activation and induces c-jun degradation in human chondrocytes: potential therapeutics for osteoarthritis, PLoS One 8 (2013) 1–12, 10.1371/journal.pone.0082033.

[79]. Zhang J, Yin J, Zhao D, Wang C, Zhang Y, Wang Y, Li T, Therapeutic effect and mechanism of action of quercetin in a rat model of osteoarthritis, J. Int. Med. Res. 48 (2019), 10.1177/0300060519873461.

[80]. Abri Aghdam M, Bagheri R, Mosafer J, Baradaran B, Hashemzaei M, Baghbanzadeh A, de la Guardia M, Mokhtarzadeh A, Recent advances on thermosensitive and pH-sensitive liposomes employed in controlled release, J. Control. Release 315 (2019) 1–22, 10.1016/j.jconrel.2019.09.018. [PubMed: 31647978]

[81]. Sarkar N, Bose S, Liposome-encapsulated curcumin-loaded 3D printed Scaffold for bone tissue engineering, ACS Appl. Mater. Interfaces 11 (2019) 17184–17192, 10.1021/acsami.9b01218. [PubMed: 30924639]

[82]. Mandal A, Bisht R, Rupenthal ID, Mitra AK, Polymeric micelles for ocular drug delivery: from structural frameworks to recent preclinical studies, J. Control. Release 248 (2017) 96–116, 10.1016/j.jconrel.2017.01.012. [PubMed: 28087407]

[83]. Xi Y, Jiang T, Yu Y, Yu J, Xue M, Xu N, Wen J, Wang W, He H, Shen Y, Chen D, Ye X, Webster TJ, Dual targeting curcumin loaded alendronatehyaluronan- octadecanoic acid micelles for improving osteosarcoma therapy, Int. J. Nanomedicine 14 (2019) 6425–6437, 10.2147/IJN.S211981. [PubMed: 31496695]

[84]. Sur S, Rathore A, Dave V, Reddy KR, Chouhan RS, Sadhu V, Recent developments in functionalized polymer nanoparticles for efficient drug delivery system, Nano-Struct. Nano-Objects. 20 (2019), 100397, 10.1016/j.nanoso.2019.100397.

[85]. Masood F, Polymeric nanoparticles for targeted drug delivery system for cancer therapy, Mater. Sci. Eng. C 60 (2016) 569–578, 10.1016/j.msec.2015.11.067.

[86]. Rahbar Takrami S, Ranji N, Sadeghizadeh M, Antibacterial effects of curcumin encapsulated in nanoparticles on clinical isolates of *Pseudomonas aeruginosa* through downregulation of efflux pumps, Mol. Biol. Rep. 46 (2019) 2395–2404, 10.1007/s11033-019-04700-2. [PubMed: 30778922]

[87]. Dreiss CA, Hydrogel design strategies for drug delivery, Curr. Opin. Colloid Interface Sci. 48 (2020) 1–17, 10.1016/j.cocis.2020.02.001.

[88]. Qureshi D, Nayak SK, Maji S, Anis A, Kim D, Pal K, Environment sensitive hydrogels for drug delivery applications, Eur. Polym. J. 120 (2019), 109220, 10.1016/j.eurpolymj.2019.109220.

[89]. Yu W, Zhu Y, Li H, He Y, Injectable quercetin-loaded hydrogel with cartilage-protection and immunomodulatory properties for articular cartilage repair, ACS Appl. Bio Mater. 3 (2020) 761–771, 10.1021/acsabm.9b00673.

[90]. Pednekar PP, Godiyal SC, Jadhav KR, Kadam VJ, Chapter 23 - Mesoporous silica nanoparticles: a promising multifunctional drug delivery system, in: Ficai A, A.M.B.T.-N. for Grumezescu CT (Eds.), Micro Nano Technol, Elsevier, 2017, pp. 593–621, 10.1016/B978-0-323-46144-3.00023-4.

[91]. Colilla M, Vallet-Regí M, Targeted stimuli-responsive mesoporous silica nanoparticles for bacterial infection treatment, Int. J. Mol. Sci. 21 (2020) 1–32, 10.3390/ijms21228605.

[92]. Wu C, Zhu Y, Wu T, Wang L, Yuan Y, Chen J, Hu Y, Pang J, Enhanced functional properties of biopolymer film incorporated with curcurmin-loaded mesoporous silica nanoparticles for food packaging, Food Chem. 288 (2019) 139–145, 10.1016/j.foodchem.2019.03.010. [PubMed: 30902273]

[93]. Bandyopadhyay A, Shivaram A, Mitra I, Bose S, Electrically polarized TiO2 nanotubes on Ti implants to enhance early-stage osseointegration, Acta Biomater. 96 (2019) 686–693, 10.1016/j.actbio.2019.07.028. [PubMed: 31326668]

[94]. Saha S, Pramanik K, Biswas A, Antibacterial activity and biocompatibility of curcumin/TiO2 nanotube array system on Ti6Al4V bone implants, Mater. Technol. 36 (2021) 221–232, 10.1080/10667857.2020.1742984.

[95]. Chavda VP, Pandya A, Kumar L, Raval N, Vora LK, Pulakkat S, Patravale V, Salwa Y, Tang Duo BZ, Exosome nanovesicles: a potential carrier for therapeutic delivery, Nano Today 49 (2023), 101771, 10.1016/j.nantod.2023.101771.

[96]. Narayanan K, Kumar S, Padmanabhan P, Gulyas B, Wan ACA, Rajendran VM, Lineage-specific exosomes could override extracellular matrix mediated human mesenchymal stem cell differentiation, Biomaterials 182 (2018) 312–322, 10.1016/j.biomaterials.2018.08.027. [PubMed: 30153612]

[97]. Cui Y, Luan J, Li H, Zhou X, Han J, Exosomes derived from mineralizing osteoblasts promote ST2 cell osteogenic differentiation by alteration of microRNA expression, FEBS Lett. 590 (2016) 185–192, 10.1002/1873-3468.12024. [PubMed: 26763102]

[98]. Huynh N, Vonmoss L, Smith D, Rahman I, Felemban MF, Zuo J, Rody WJ, McHugh KP, Holliday LS, Characterization of regulatory extracellular vesicles from osteoclasts, J. Dent. Res. 95 (2016) 673–679, 10.1177/0022034516633189. [PubMed: 26908631]

[99]. De Jonge LT, Leeuwenburgh SCG, Wolke JGC, Jansen JA, Organic-inorganic surface modifications for titanium implant surfaces, Pharm. Res. 25 (2008) 2357–2369, 10.1007/s11095-008-9617-0. [PubMed: 18509601]

[100]. Seif S, Franzen L, Windbergs M, Overcoming drug crystallization in electrospun fibers - Elucidating key parameters and developing strategies for drug delivery, Int. J. Pharm. 478 (2015) 390–397, 10.1016/j.ijpharm.2014.11.045. [PubMed: 25448563]

[101]. Seoane-Viaño I, Januskaite P, Alvarez-Lorenzo C, Basit AW, Goyanes A, Semi-solid extrusion 3D printing in drug delivery and biomedicine: personalised solutions for healthcare challenges, J. Control. Release 332 (2021) 367–389, 10.1016/j.jconrel.2021.02.027. [PubMed: 33652114]

[102]. Khakestani M, Jafari SH, Zahedi P, Bagheri R, Hajiaghaee R, Physical, morphological, and biological studies on PLA/nHA composite nanofibrous webs containing *Equisetum arvense* herbal extract for bone tissue engineering, J. Appl. Polym. Sci. 134 (2017) 1–10, 10.1002/app.45343.

[103]. Kashte S, Dhumal R, Chaudhary P, Sharma RK, Dighe V, Kadam S, Bone regeneration in critical-size calvarial defect using functional biocompatible osteoinductive herbal scaffolds and human umbilical cord Wharton's Jelly-derived mesenchymal stem cells, Mater. Today Commun. 26 (2021), 102049, 10.1016/j.mtcomm.2021.102049.

[104]. Baniasadi H, Ajdary R, Trifol J, Rojas OJ, Seppälä J, Direct ink writing of *aloe vera*/cellulose nanofibrils bio-hydrogels, Carbohydr. Polym. 266 (2021), 10.1016/j.carbpol.2021.118114.

[105]. Dorj B, Won JE, Purevdorj O, Patel KD, Kim JH, Lee EJ, Kim HW, A novel therapeutic design of microporous-structured biopolymer scaffolds for drug loading and delivery, Acta Biomater. 10 (2014) 1238–1250, 10.1016/j.actbio.2013.11.002. [PubMed: 24239677]

[106]. Bose S, Sarkar N, Natural medicinal compounds in bone tissue engineering, Trends Biotechnol. 38 (2020) 404–417, 10.1016/j.tibtech.2019.11.005. [PubMed: 31882304]

[107]. Matsumoto T, Okazaki M, Inoue M, Yamaguchi S, Kusunose T, Toyonaga T, Hamada Y, Takahashi J, Hydroxyapatite particles as a controlled release carrier of protein, Biomaterials. 25 (2004) 3807–3812, 10.1016/j.biomaterials.2003.10.081. [PubMed: 15020156]

[108]. Diaz-Rodriguez P, Sánchez M, Landin M, Drug-loaded biomimetic ceramics for tissue engineering, Pharmaceutics. 10 (2018) 1–20, 10.3390/pharmaceutics10040272.

[109]. Thomazeau H, Langlais F, Antibiotic release by tricalcic phosphate bone implantation. In vitro and in vivo pharmacokinetics of different galenic forms, Chirurgie. 121 (1997) 663–666, http://europepmc.org/abstract/MED/9138328. [PubMed: 9138328]

[110]. Chai F, Hornez J-C, Blanchemain N, Neut C, Descamps M, Hildebrand HF, Antibacterial activation of hydroxyapatite (HA) with controlled porosity by different antibiotics, Biomol. Eng. 24 (2007) 510–514, 10.1016/j.bioeng.2007.08.001. [PubMed: 17869175]

[111]. Dong X, Wang Q, Wu T, Pan H, Understanding adsorption-desorption dynamics of BMP-2 on hydroxyapatite (001) surface, Biophys. J. 93 (2007) 750–759, 10.1529/biophysj.106.103168. [PubMed: 17617550]

[112]. Palazzo B, Iafisco M, Laforgia M, Margiotta N, Natile G, Bianchi CL, Walsh D, Mann S, Roveri N, Biomimetic hydroxyapatite-drug nanocrystals as potential bone substitutes with antitumor drug delivery properties, Adv. Funct. Mater. 17 (2007) 2180–2188, 10.1002/adfm.200600361.

[113]. Cao L, Yu Y, Wang J, Werkmeister JA, McLean KM, Liu C, 2-N, 6-O-sulfated chitosan-assisted BMP-2 immobilization of PCL scaffolds for enhanced osteoinduction, Mater. Sci. Eng. C 74 (2017) 298–306, 10.1016/j.msec.2016.12.004.

[114]. Cosijns A, Vervaet C, Luyten J, Mullens S, Siepmann F, Van Hoorebeke L, Masschaele B, Cnudde V, Remon JP, Porous hydroxyapatite tablets as carriers for low-dosed drugs, Eur. J. Pharm. Biopharm. 67 (2007) 498–506, 10.1016/j.ejpb.2007.02.018. [PubMed: 17407810]

[115]. Kandori K, Mukai M, Fujiwara A, Yasukawa A, Ishikawa T, Adsorption of bovine serum albumin and lysozyme on hydrophobic calcium hydroxyapatites, J. Colloid Interface Sci. 212 (1999) 600–603, 10.1006/jcis.1998.6060. [PubMed: 10092395]

[116]. Banerjee SS, Bandyopadhyay A, Bose S, Biphasic resorbable calcium phosphate ceramic for bone implants and local alendronate delivery, Adv. Eng. Mater. 12 (2010) B148–B155, 10.1002/adem.200980072.

[117]. Josse S, Faucheux C, Soueidan A, Grimandi G, Massiot D, Alonso B, Janvier P, Laïb S, Pilet P, Gauthier O, Daculsi G, Guicheux J, Bujoli B, Bouler JM, Novel biomaterials for bisphosphonate delivery, Biomaterials. 26 (2005) 2073–2080, 10.1016/j.biomaterials.2004.05.019. [PubMed: 15576181]

[118]. Dutta S, Das Gupta D, Conjugation of Ibuprofen to Poly Ethylene Glycol and In-vitro drug release evaluation, J. Drug Deliv. Ther. 9 (2019) 110–115. http://www.jddtonline.info/index.php/jddt/article/view/2953.

[119]. Huang X, Brazel CS, On the importance and mechanisms of burst release in matrix-controlled drug delivery systems, J. Control. Release 73 (2001) 121–136, 10.1016/S0168-3659(01)00248-6. [PubMed: 11516493]

[120]. Rambhia KJ, Ma PX, Controlled drug release for tissue engineering, J. Control. Release 219 (2015) 119–128, 10.1016/j.jconrel.2015.08.049. [PubMed: 26325405]

[121]. Robertson SF, Bose S, Enhanced osteogenesis of 3D printed β-TCP scaffolds with Cissus Quadrangularis extract-loaded polydopamine coatings, J. Mech. Behav. Biomed. Mater. 111 (2020), 103945, 10.1016/j.jmbbm.2020.103945. [PubMed: 32920263]

[122]. Bose S, Banerjee D, Vu AA, Ginger and garlic extracts enhance osteogenesis in 3D printed calcium phosphate bone scaffolds with bimodal pore distribution, ACS Appl. Mater. Interfaces 14 (2022) 12964–12975, 10.1021/acsami.1c19617. [PubMed: 35263096]

[123]. Bose S, Sarkar N, Banerjee D, Effects of PCL, PEG and PLGA polymers on curcumin release from calcium phosphate matrix for in vitro and in vivo bone regeneration, Mater. Today Chem. 8 (2018) 110–120, 10.1016/j.mtchem.2018.03.005. [PubMed: 30480167]

[124]. Rauschmann MA, Wichelhaus TA, Stirnal V, Dingeldein E, Zichner L, Schnettler R, Alt V, Nanocrystalline hydroxyapatite and calcium sulphate as biodegradable composite carrier material for local delivery of antibiotics in bone infections, Biomaterials. 26 (2005) 2677–2684, 10.1016/j.biomaterials.2004.06.045. [PubMed: 15585271]

[125]. Ferraz MP, Mateus AY, Sousa JC, Monteiro FJ, Nanohydroxyapatite microspheres as delivery system for antibiotics: release kinetics, antimicrobial activity, and interaction with osteoblasts, J. Biomed. Mater. Res. Part A. 81A (2007) 994–1004, 10.1002/JBM.A.31151.

[126]. Fina F, Goyanes A, Madla CM, Awad A, Trenfield SJ, Kuek JM, Patel P, Gaisford S, Basit AW, 3D printing of drug-loaded gyroid lattices using selective laser sintering, Int. J. Pharm. 547 (2018) 44–52, 10.1016/j.ijpharm.2018.05.044. [PubMed: 29787894]

[127]. Chen Y, Liu X, Liu R, Gong Y, Wang M, Huang Q, Feng Q, Yu B, Zero-order controlled release of BMP2-derived peptide P24 from the chitosan scaffold by chemical grafting modification technique for promotion of osteogenesis in vitro and enhancement of bone repair in vivo, Theranostics. 7 (2017) 1072–1087, 10.7150/thno.18193. [PubMed: 28435449]

[128]. Liu Y, De Groot K, Hunziker EB, BMP-2 liberated from biomimetic implant coatings induces and sustains direct ossification in an ectopic rat model, Bone. 36 (2005) 745–757, 10.1016/j.bone.2005.02.005. [PubMed: 15814303]

[129]. Kazemzadeh-Narbat M, Lai BFL, Ding C, Kizhakkedathu JN, Hancock REW, Wang R, Multilayered coating on titanium for controlled release of antimicrobial peptides for the prevention of implant-associated infections, Biomaterials. 34 (2013) 5969–5977, 10.1016/j.biomaterials.2013.04.036. [PubMed: 23680363]

[130]. Tarafder S, Nansen K, Bose S, Lovastatin release from polycaprolactone coated β-tricalcium phosphate: Effects of pH, concentration and drug-polymer interactions, Mater. Sci. Eng. C 33 (2013) 3121–3128, 10.1016/j.msec.2013.02.049.

[131]. Vu AA, Bose S, Effects of vitamin D3 release from 3D printed calcium phosphate scaffolds on osteoblast and osteoclast cell proliferation for bone tissue engineering, RSC Adv. 9 (2019) 34847–34853, 10.1039/c9ra06630f. [PubMed: 35474960]

[132]. Buket Basmanav F, Kose GT, Hasirci V, Sequential growth factor delivery from complexed microspheres for bone tissue engineering, Biomaterials. 29 (2008) 4195–4204, 10.1016/j.biomaterials.2008.07.017. [PubMed: 18691753]

[133]. Patil SD, Papadmitrakopoulos F, Burgess DJ, Concurrent delivery of dexamethasone and VEGF for localized inflammation control and angiogenesis, J. Control. Release 117 (2007) 68–79, 10.1016/j.jconrel.2006.10.013. [PubMed: 17169457]

[134]. Rowe CW, Katstra WE, Palazzolo RD, Giritlioglu B, Teung P, Cima MJ, Multimechanism oral dosage forms fabricated by three dimensional printing(TM), J. Control. Release 66 (2000) 11–17, 10.1016/S0168-3659(99)00224-2. [PubMed: 10708874]

[135]. Wu W, Zheng Q, Guo X, Sun J, Liu Y, A programmed release multi-drug implant fabricated by three-dimensional printing technology for bone tuberculosis therapy, Biomed. Mater. 4 (2009), 10.1088/1748-6041/4/6/065005.

[136]. Roy M, Bandyopadhyay A, Bose S, Chapter 6 - Ceramics in Bone Grafts and Coated Implants, Elsevier Inc., 2017, pp. 265–314, 10.1016/B978-0-12-802792-9.00006-9.

[137]. Chen YW, Moussi J, Drury JL, Wataha JC, Zirconia in biomedical applications, Exp. Rev. Med. Dev. 13 (10) (2016).

[138]. Tarafder S, Balla VK, Davies NM, Bandyopadhyay A, Bose S, Microwave-sintered 3D printed tricalcium phosphate scaffolds for bone tissue engineering, J. Tissue Eng. Regen. Med. 7 (2013) 631–641, 10.1002/term.555. [PubMed: 22396130]

[139]. Dasgupta S, Tarafder S, Bandyopadhyay A, Bose S, Effect of grain size on mechanical, surface and biological properties of microwave sintered hydroxyapatite, Mater. Sci. Eng. C 33 (2013) 2846–2854, 10.1016/j.msec.2013.03.004.

[140]. Vahabzadeh S, Roy M, Bandyopadhyay A, Bose S, Phase stability and biological property evaluation of plasma sprayed hydroxyapatite coatings for orthopedic and dental applications, Acta Biomater. 17 (2015) 47–55, 10.1016/j.actbio.2015.01.022. [PubMed: 25638672]

[141]. Roy M, Balla VK, Bandyopadhyay A, Bose S, Compositionally graded hydroxyapatite/tricalcium phosphate coating on Ti by laser and induction plasma, Acta Biomater. 7 (2011) 866–873, 10.1016/j.actbio.2010.09.016. [PubMed: 20854939]

[142]. Bose S, Vahabzadeh S, Bandyopadhyay A, Bone tissue engineering using 3D printing, Mater. Today 16 (2013) 496–504, 10.1016/j.mattod.2013.11.017.

[143]. Tarafder S, Bose S, Polycaprolactone-coated 3D printed tricalcium phosphate scaffolds for bone tissue engineering: *In vitro* alendronate release behavior and local delivery effect on *in vivo* osteogenesis, ACS Appl. Mater. Interfaces 6 (2014) 9955–9965, 10.1021/am501048n. [PubMed: 24826838]

[144]. Miao Y, Chen Y, Liu X, Diao J, Zhao N, Shi X, Wang Y, Melatonin decorated 3D-printed beta-tricalcium phosphate scaffolds promoting bone regeneration in a rat calvarial defect model, J. Mater. Chem. B 7 (2019) 3250–3259, 10.1039/c8tb03361g.

[145]. Akkineni AR, Luo Y, Schumacher M, Nies B, Lode A, Gelinsky M, 3D plotting of growth factor loaded calcium phosphate cement scaffolds, Acta Biomater. 27 (2015) 264–274, 10.1016/j.actbio.2015.08.036. [PubMed: 26318366]

[146]. Kim BS, Yang SS, Kim CS, Incorporation of BMP-2 nanoparticles on the surface of a 3D-printed hydroxyapatite scaffold using an ε-polycaprolactone polymer emulsion coating method for bone tissue engineering, Colloids Surf. B: Biointerfaces 170 (2018) 421–429, 10.1016/j.colsurfb.2018.06.043. [PubMed: 29957531]

[147]. Liu X, Ma PX, Polymeric Scaffolds for bone tissue engineering, Ann. Biomed. Eng. 32 (2004) 477–486, 10.1023/B:ABME.0000017544.36001.8e. [PubMed: 15095822]

[148]. Bose S, Koski C, Vu AA, Additive manufacturing of natural biopolymers and composites for bone tissue engineering, Mater. Horizons. 7 (2020) 211–227, 10.1039/d0mh00277a.

[149]. Guo L, Liang Z, Yang L, Du W, Yu T, Tang H, Li C, Qiu H, The role of natural polymers in bone tissue engineering, J. Control. Release 338 (2021) 571–582, 10.1016/J.JCONREL.2021.08.055. [PubMed: 34481026]

[150]. Ge Z, Tian X, Heng BC, Fan V, Yeo JF, Cao T, Histological evaluation of osteogenesis of 3D-printed poly-lactic-co-glycolic acid (PLGA) scaffolds in a rabbit model, Biomed. Mater. 4 (2009), 021001, 10.1088/1748-6041/4/2/021001. [PubMed: 19208943]

[151]. Dash TK, Konkimalla VB, Poly-ε-caprolactone based formulations for drug delivery and tissue engineering: a review, J. Control. Release 158 (2012) 15–33, 10.1016/j.jconrel.2011.09.064. [PubMed: 21963774]

[152]. Yang F, Wang J, Hou J, Guo H, Liu C, Bone regeneration using cell-mediated responsive degradable PEG-based scaffolds incorporating with rhBMP-2, Biomaterials. 34 (2013) 1514–1528, 10.1016/J.BIOMATERIALS.2012.10.058. [PubMed: 23187021]

[153]. Anseth KS, Shastri VR, Langer R, Photopolymerizable degradable polyanhydrides with osteocompatibility, Nat. Biotechnol. 17 (1999).

[154]. James K, Levene H, Russell Parsons J, Kohn J, Small changes in polymer chemistry have a large effect on the bone-implant interface: evaluation of a series of degradable tyrosine-derived polycarbonates in bone defects, Biomaterials. 20 (1999) 2203–2212, 10.1016/S0142-9612(99)00151-9. [PubMed: 10614927]

[155]. Martina M, Hutmacher DW, Biodegradable polymers applied in tissue engineering research: a review, Polym. Int. 56 (2007) 145–157, 10.1002/PI.2108.

[156]. Yan Y, Chen H, Zhang H, Guo C, Yang K, Chen K, Cheng R, Qian N, Sandler N, Zhang YS, Shen H, Qi J, Cui W, Deng L, Vascularized 3D printed scaffolds for promoting bone regeneration, Biomaterials. 190–191 (2019) 97–110, 10.1016/j.biomaterials.2018.10.033.

[157]. Lee SJ, Lee D, Yoon TR, Kim HK, Jo HH, Park JS, Lee JH, Kim WD, Kwon IK, Park SA, Surface modification of 3D-printed porous scaffolds *via* mussel-inspired polydopamine and effective immobilization of rhBMP-2 to promote osteogenic differentiation for bone tissue engineering, Acta Biomater. 40 (2016) 182–191, 10.1016/j.actbio.2016.02.006. [PubMed: 26868173]

[158]. Park SA, Lee SH, Kim WD, Fabrication of porous polycaprolactone/hydroxyapatite (PCL/HA) blend scaffolds using a 3D plotting system for bone tissue engineering, Bioprocess Biosyst. Eng. 34 (2011) 505–513, 10.1007/s00449-010-0499-2. [PubMed: 21170553]

[159]. Babilotte J, Martin B, Guduric V, Bareille R, Agniel R, Roques S, Héroguez V, Dussauze M, Gaudon M, Le Nihouannen D, Catros S, Development and characterization of a PLGA-HA composite material to fabricate 3D-printed scaffolds for bone tissue engineering, Mater. Sci. Eng. C 118 (2021), 111334, 10.1016/J.MSEC.2020.111334.

[160]. Raghavendran HRB, Mohan S, Genasan K, Murali MR, Naveen SV, Talebian S, McKean R, Kamarul T, Synergistic interaction of platelet derived growth factor (PDGF) with the surface of PLLA/Col/HA and PLLA/HA scaffolds produces rapid osteogenic differentiation, Colloids Surf. B: Biointerfaces 139 (2016) 68–78, 10.1016/j.colsurfb.2015.11.053. [PubMed: 26700235]

[161]. Oh SH, An DB, Kim TH, Lee JH, Wide-range stiffness gradient PVA/HA hydrogel to investigate stem cell differentiation behavior, Acta Biomater. 35 (2016) 23–31, 10.1016/J.ACTBIO.2016.02.016. [PubMed: 26883774]

[162]. Kalita SJ, Bose S, Hosick HL, Bandyopadhyay A, Development of controlled porosity polymer-ceramic composite scaffolds *via* fused deposition modeling, Mater. Sci. Eng. C 23 (2003) 611–620, 10.1016/S0928-4931(03)00052-3.

[163]. Bandyopadhyay A, Ciliveri S, Bose S, Metal additive manufacturing for load-bearing implants, J. Indian Inst. Sci. 102 (2022) 561–584, 10.1007/s41745-021-00281-x.

[164]. Bandyopadhyay A, Espana F, Balla VK, Bose S, Ohgami Y, Davies NM, Influence of porosity on mechanical properties and *in vivo* response of Ti6Al4V implants, Acta Biomater. 6 (2010) 1640–1648, 10.1016/J.ACTBIO.2009.11.011. [PubMed: 19913643]

[165]. Bandyopadhyay A, Mitra I, Goodman SB, Kumar M, Progress in materials science improving biocompatibility for next generation of metallic implants, Prog. Mater. Sci. 133 (2023), 101053, 10.1016/j.pmatsci.2022.101053. [PubMed: 36686623]

[166]. Roy M, Vamsi Krishna B, Bandyopadhyay A, Bose S, Laser processing of bioactive tricalcium phosphate coating on titanium for load-bearing implants, Acta Biomater. 4 (2008) 324–333, 10.1016/j.actbio.2007.09.008. [PubMed: 18039597]

[167]. Bose S, Banerjee D, Shivaram A, Tarafder S, Bandyopadhyay A, Calcium phosphate coated 3D printed porous titanium with nanoscale surface modification for orthopedic and dental applications, Mater. Des. 151 (2018) 102–112, 10.1016/j.matdes.2018.04.049. [PubMed: 31406392]

[168]. Roy M, Fielding GA, Beyenal H, Bandyopadhyay A, Bose S, Mechanical, *In vitro* Antimicrobial, and biological properties of plasma-sprayed silver-doped hydroxyapatite coating, ACS Appl. Mater. Interfaces 4 (2012) 1341–1349, 10.1021/am201610q. [PubMed: 22313742]

[169]. Fielding GA, Roy MM, Bandyopadhyay AA, Bose SS, Antibacterial and biological characteristics of plasma sprayed silver and strontium doped hydroxyapatite coatings, Acta Biomater. 8 (2012) 3144–3152, 10.1016/j.actbio.2012.04.004. [PubMed: 22487928]

[170]. Vu AA, Robertson SF, Ke D, Bandyopadhyay A, Bose S, Mechanical and biological properties of ZnO, SiO2, and Ag2O doped plasma sprayed hydroxyapatite coating for orthopedic and dental applications, Acta Biomater. 92 (2019) 325–335, 10.1016/j.actbio.2019.05.020. [PubMed: 31082568]

[171]. Fischer NG, Münchow EA, Tamerler C, Bottino MC, Aparicio C, Harnessing biomolecules for bioinspired dental biomaterials, J. Mater. Chem. B 8 (2020) 8713–8747, 10.1039/d0tb01456g. [PubMed: 32747882]

[172]. Izquierdo-Barba I, Santos-Ruiz L, Becerra J, Feito MJ, Fernández-Villa D, Serrano MC, Díaz-Güemes I, Fernández-Tomé B, Enciso S, Sánchez-Margallo FM, Monopoli D, Afonso H, Portolés MT, Arcos D, Vallet-Regí M, Synergistic effect of Si-hydroxyapatite coating and VEGF adsorption on Ti6Al4V-ELI scaffolds for bone regeneration in an osteoporotic bone environment, Acta Biomater. 83 (2019) 456–466, 10.1016/J.ACTBIO.2018.11.017. [PubMed: 30445158]

[173]. Qing Y, Li K, Li D, Qin Y, Antibacterial effects of silver incorporated zeolite coatings on 3D printed porous stainless steels, Mater. Sci. Eng. C 108 (2020), 110430, 10.1016/j.msec.2019.110430.

[174]. Das K, Bose S, Bandyopadhyay A, Karandikar B, Gibbins BL, Surface coatings for improvement of bone cell materials and antimicrobial activities of Ti implants, J. Biomed. Mater. Res. Part B Appl. Biomater. 87 (2008) 455–460, 10.1002/jbm.b.31125.

[175]. Mani G, Johnson DM, Marton D, Feldman MD, Patel D, Ayon AA, Agrawal CM, Drug delivery from gold and titanium surfaces using self-assembled monolayers, Biomaterials. 29 (2008) 4561–4573, 10.1016/J.BIOMATERIALS.2008.08.014. [PubMed: 18790530]

[176]. Horcajada P, Chalati T, Serre C, Gillet B, Sebrie C, Baati T, Eubank JF, Heurtaux D, Clayette P, Kreuz C, Chang JS, Hwang YK, Marsaud V, Bories PN, Cynober L, Gil S, Férey G, Couvreur P, Gref R, Porous metal-organic-framework nanoscale carriers as a potential platform for drug deliveryand imaging, Nat. Mater. 9 (2010) 172–178, 10.1038/nmat2608. [PubMed: 20010827]

[177]. Yazici H, Habib G, Boone K, Urgen M, Utku FS, Tamerler C, Self-assembling antimicrobial peptides on nanotubular titanium surfaces coated with calcium phosphate for local therapy, Mater. Sci. Eng. C 94 (2019) 333–343, 10.1016/j.msec.2018.09.030.

[178]. Aghion E, Yered T, Perez Y, Gueta Y, The prospects of carrying and releasing drugs *via* biodegradable magnesium foam, Adv. Eng. Mater. 12 (2010), 10.1002/ADEM.200980044.

[179]. Gimeno M, Pinczowski P, Pérez M, Giorello A, Martínez MÁ, Santamaría J, Arruebo M, Luján L, A controlled antibiotic release system to prevent orthopedic-implant associated infections: an *in vitro* study, Eur. J. Pharm. Biopharm. 96 (2015) 264, 10.1016/J.EJPB.2015.08.007. [PubMed: 26297104]

[180]. Kwon BJ, Seon GM, Lee MH, Koo MA, Kim MS, Kim D, Han JJ, Kim D, Kim J, Park JC, Locally delivered ethyl-2,5-dihydroxybenzoate using 3D printed bone implant for promotion of bone regeneration in a osteoporotic animal model, Eur. Cells Mater. 35 (2018) 1–12, 10.22203/eCM.v035a01.

[181]. Jia Z, Zhou W, Yan J, Xiong P, Guo H, Cheng Y, Zheng Y, Constructing multilayer silk protein/nanosilver biofunctionalized hierarchically structured 3D printed Ti6Al4 v Scaffold for repair of infective bone defects, ACS Biomater. Sci. Eng. 5 (2019) 244–261, 10.1021/acsbiomaterials.8b00857. [PubMed: 33405864]

[182]. Li Y, Li L, Ma Y, Zhang K, Li G, Lu B, Lu C, Chen C, Wang L, Wang H, Cui X, 3D-printed Titanium cage with PVA-vancomycin coating prevents surgical site infections (SSIs), Macromol. Biosci. 20 (2020), 10.1002/mabi.201900394.

[183]. Jang CH, Lee JU, Kim GH, Synergistic effect of alginate/BMP-2/Umbilical cord serum-coated on 3D-printed PCL biocomposite for mastoid obliteration model, J. Ind. Eng. Chem. 72 (2019) 432–441, 10.1016/j.jiec.2018.12.046.

[184]. Kim SE, Yun YP, Shim KS, Kim HJ, Park K, Song HR, 3D printed alendronate-releasing poly(caprolactone) porous scaffolds enhance osteogenic differentiation and bone formation in rat tibial defects, Biomed. Mater. 11 (2016), 10.1088/1748-6041/11/5/055005.

[185]. Bai J, Wang H, Gao W, Liang F, Wang Z, Zhou Y, Lan X, Chen X, Cai N, Huang W, Tang Y, Melt electrohydrodynamic 3D printed poly (ε-caprolactone)/polyethylene glycol/roxithromycin scaffold as a potential anti-infective implant in bone repair, Int. J. Pharm. 576 (2020), 118941, 10.1016/j.ijpharm.2019.118941. [PubMed: 31881261]

[186]. Sun M, Chen M, Wang M, Hansen J, Baatrup A, Dagnaes-Hansen F, Rölfing JHD, Jensen J, Lysdahl H, Li H, Johannsen M, Le DQS, Kjems J, Bünger CE, In vivo drug release behavior and osseointegration of a doxorubicin-loaded tissue-engineered scaffold, RSC Adv. 6 (2016) 76237–76245, 10.1039/c6ra05351c.

[187]. Zhang ZZ, Zhang HZ, Zhang ZY, 3D printed poly(ε-caprolactone) scaffolds function with simvastatin-loaded poly(lactic-co-glycolic acid) microspheres to repair load-bearing segmental bone defects, Exp. Ther. Med. 17 (2019) 79–90, 10.3892/etm.2018.6947. [PubMed: 30651767]

[188]. Wang H, Wu G, Zhang J, Zhou K, Yin B, Su X, Qiu G, Yang G, Zhang X, Zhou G, Wu Z, Osteogenic effect of controlled released rhBMP-2 in 3D printed porous hydroxyapatite scaffold, Colloids Surf. B: Biointerfaces 141 (2016) 491–498, 10.1016/j.colsurfb.2016.02.007. [PubMed: 26896655]

[189]. Ishack S, Mediero A, Wilder T, Ricci JL, Cronstein BN, Bone regeneration in critical bone defects using three-dimensionally printed β-tricalcium phosphate/hydroxyapatite scaffolds is enhanced by coating scaffolds with either dipyridamole or BMP-2, J. Biomed. Mater. Res. Part B Appl. Biomater. 105 (2017) 366–375, 10.1002/jbm.b.33561.

[190]. Strobel L, Rath S, Maier A, Beier J, Arkudas A, Greil P, Horch R, Kneser U, Induction of bone formation in biphasic calcium phosphate scaffolds by bone morphogenetic protein-2 and primary osteoblasts, J. Tissue Eng. Regen. Med. 8 (2014) 176–185, 10.1002/TERM.1511. [PubMed: 22740314]

[191]. Jo Y, Sarkar N, Bose S, In vitro biological evaluation of epigallocatechin gallate (EGCG) release from three-dimensional printed (3DP) calcium phosphate bone scaffolds, J. Mater. Chem. B 11 (2022) 5503–5513, 10.1039/d2tb02210a.

[192]. Bao X, Zhu L, Huang X, Tang D, He D, Shi J, Xu G, 3D biomimetic artificial bone scaffolds with dual-cytokines spatiotemporal delivery for large weight-bearing bone defect repair, Sci. Rep. 7 (2017) 1–13, 10.1038/s41598-017-08412-0. [PubMed: 28127051]

[193]. Ye L, Wang J, Liao C, Li S, Fang Y, Yang Z, Hu Y, Guo B, 3D printed composite scaffolds incorporating ruthenium complex–loaded liposomes as a delivery system to prevent the proliferation of MG-63 cells, Macromol. Mater. Eng. 304 (2019) 1–10, 10.1002/mame.201900295.

[194]. Charen E, Harbord N, Toxicity of herbs, vitamins, and supplements, Adv. Chronic Kidney Dis. 27 (2020) 67–71, 10.1053/j.ackd.2019.08.003. [PubMed: 32147004]

[195]. Yang Y, Zhang Z, Li S, Ye X, Li X, He K, Synergy effects of herb extracts: Pharmacokinetics and pharmacodynamic basis, Fitoterapia. 92 (2014) 133–147, 10.1016/j.fitote.2013.10.010. [PubMed: 24177191]

[196]. Xiao D, Liu Z, Zhang S, Zhou M, He F, Zou M, Peng J, Xie X, Liu Y, Peng D, Berberine derivatives with different pharmacological activities via structural modifications, mini-reviews, Med. Chem. 18 (2018) 1424–1441, 10.2174/1389557517666170321103139.

[197]. Tang W, Yang Y, Zhang F, Li YC, Zhou R, Wang JX, Zhu YN, Li XY, Yang YF, Zuo JP, Prevention of graft-versus-host disease by a novel immunosuppressant, (5R)-5-hydroxytriptolide (LLDT-8), through expansion of regulatory T cells, Int. Immunopharmacol. 5 (2005) 1904–1913, 10.1016/j.intimp.2005.06.010. [PubMed: 16275625]

[198]. Wang S, Hu Y, Tan W, Wu X, Chen R, Cao J, Chen M, Wang Y, Compatibility art of traditional Chinese medicine: from the perspective of herb pairs, J. Ethnopharmacol. 143 (2012) 412–423, 10.1016/j.jep.2012.07.033. [PubMed: 22871585]

[199]. Kim H, Hughes PJ, Hawes EM, Adverse events associated with metal contamination of traditional Chinese medicines in Korea: a clinical review, Yonsei, Med. J. 55 (2014) 1177–1186, 10.3349/ymj.2014.55.5.1177. [PubMed: 25048473]

[200]. FDA, Technical Considerations for Additive Manufactured Medical Devices. https://www.fda.gov/regulatory-information/%0Asearch-fda-guidance-documents/technical-considerationsadditive-%0Amanufactured-medical-devices, 2017.

[201]. Ghelich P, Kazemzadeh-Narbat M, Hassani Najafabadi A, Samandari M, Memić A, Tamayol A, (Bio)manufactured solutions for treatment of bone defects with an emphasis on US-FDA regulatory science perspective, Adv. NanoBiomed. Res. 2 (2022) 2100073, 10.1002/anbr.202100073. [PubMed: 35935166]

[202]. Gillman CE, Jayasuriya AC, FDA-approved bone grafts and bone graft substitute devices in bone regeneration, Mater. Sci. Eng. C 130 (2021), 112466, 10.1016/j.msec.2021.112466.

[203]. Bose S, Robertson SF, Vu AA, Garlic extract enhances bioceramic bone scaffolds through upregulating ALP & BGLAP expression in hMSC-monocyte co-culture, Biomater. Adv. 154 (2023) 213622, 10.1016/j.bioadv.2023.213622. [PubMed: 37742556]

[204]. Bose S, Sarkar N, Majumdar U, Micelle encapsulated curcumin and piperine-laden 3D printed calcium phosphate scaffolds enhance *in vitro* biological properties, Colloids Surf. B: Biointerfaces 231 (2023) 113563, 10.1016/j.colsurfb.2023.113563. [PubMed: 37832173]

[205]. Bhattacharjee A, Jo Y, Bose S, In vivo and In vitro properties evaluation of curcumin loaded MgO doped 3D printed TCP scaffolds, J. Mater. Chem. B 11 (21) (2023) 4725–4739. [PubMed: 37171110]

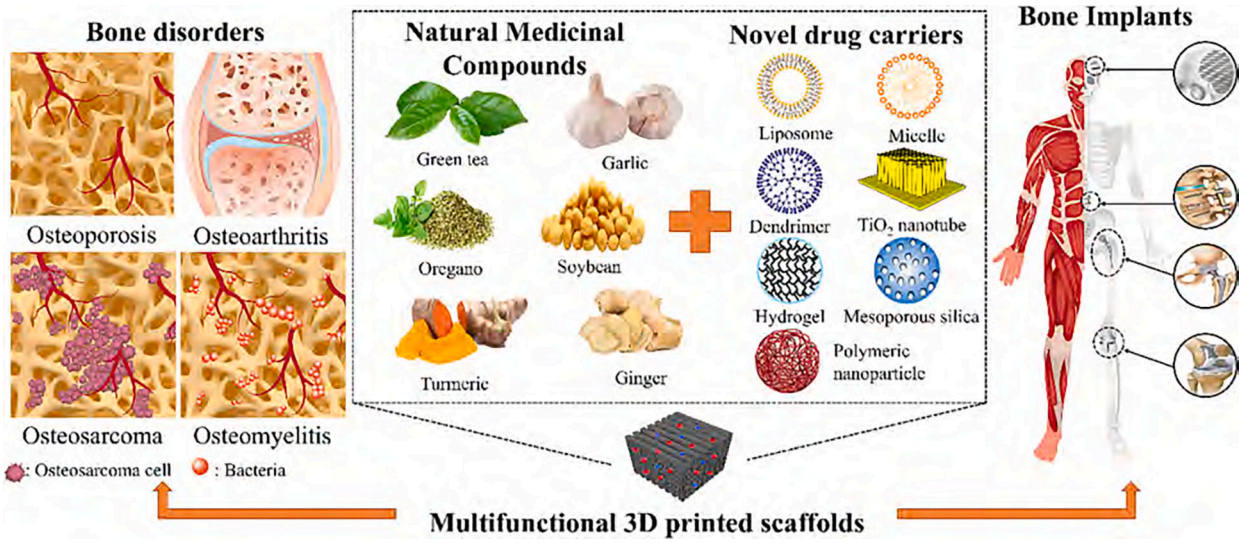


**Fig. 1.**

Multifunctional 3D printed scaffolds incorporated with natural medicinal compounds (NMCs) and drug delivery vehicles as a bone-targeted local drug delivery system for controlled and sustained delivery of NMCs to treat, control, or prevent several bone disorders, with minimized tissue toxicity.

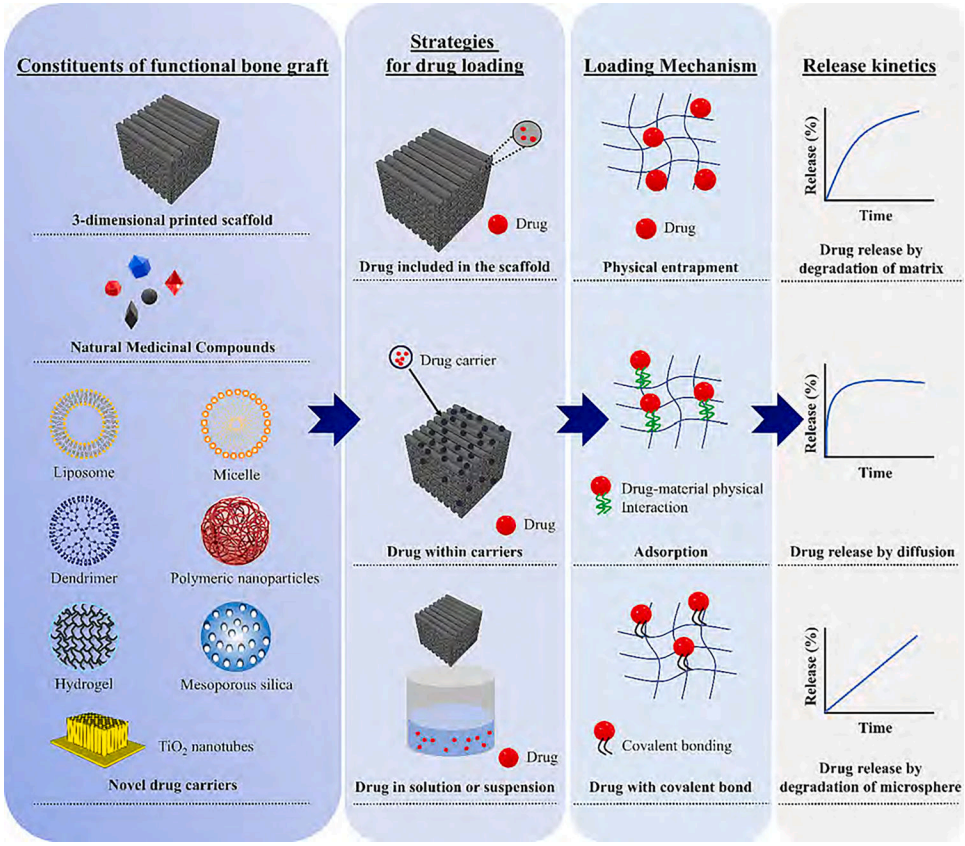


**Fig. 2.**

Strategies for drug loading and release from 3D printed bone scaffold.

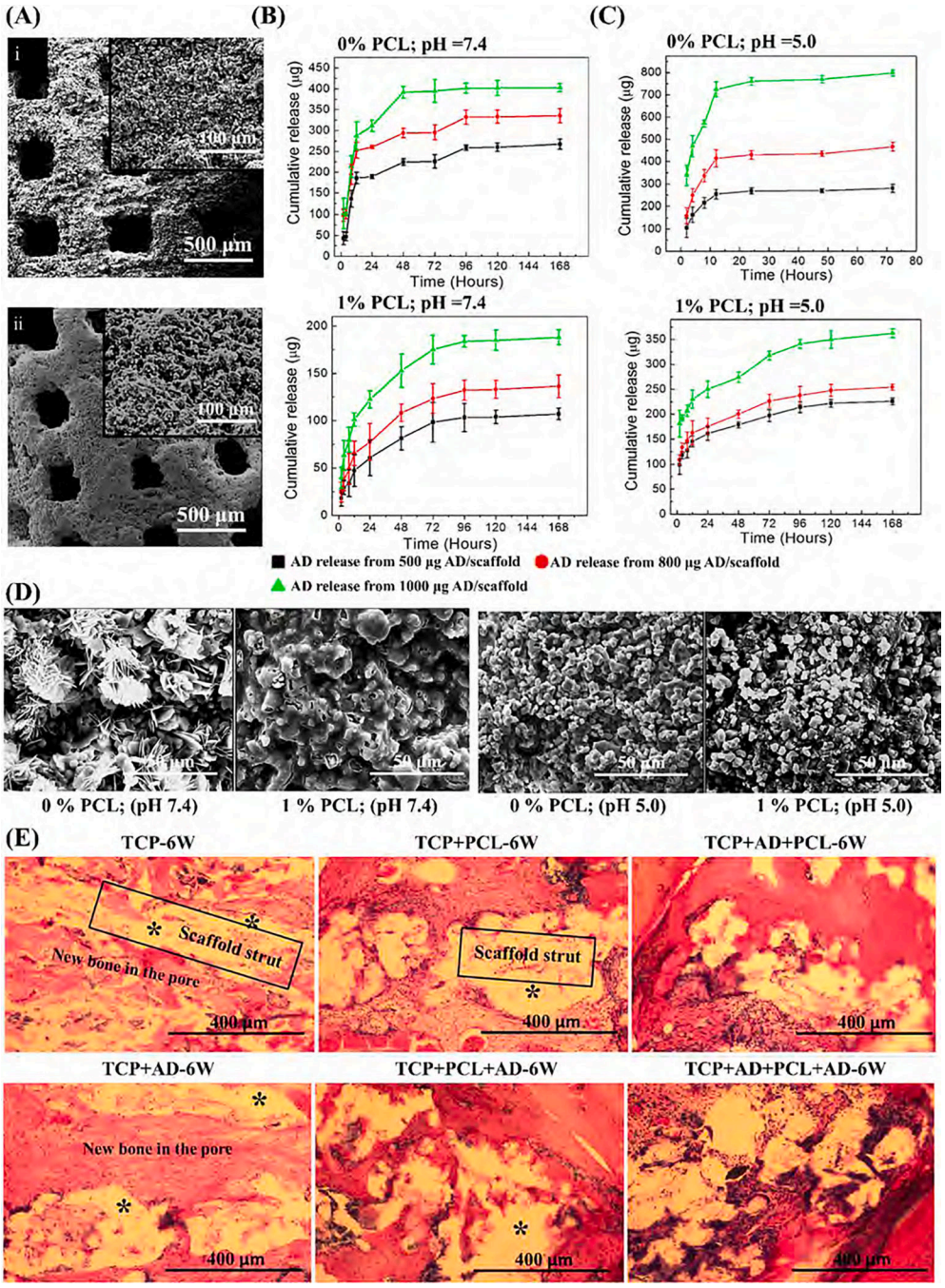


**Fig. 3.**

*In vivo* biological evaluation of controlled alendronate (AD) release from 3D printed ceramic scaffolds. (A) SEM images of (i) tricalcium phosphate (TCP) scaffold and (ii) polycaprolactone (PCL) coated TCP scaffold. (B) and (C) AD release from 3D printed TCP with and without PCL coating at pH 7.4 and pH 5.0, respectively. (D) SEM images of the surface morphology of the scaffolds at pH 7.4 and 5.0 after 7 days. (E) Hematoxylin and eosin (H&E) stained sections after 6 weeks. The asterisk (*) indicates the scaffold. Reproduced with permission [143] Copyright 2014, American Chemical Society.

SEM, scanning electron microscopy; PCL, polycaprolactone; AD, alendronate; TCP, tricalcium phosphate; TCP + PCL, control TCP and PCL coated TCP scaffolds; TCP + PCL + AD, AD-loaded TCP scaffolds with PCL coating.

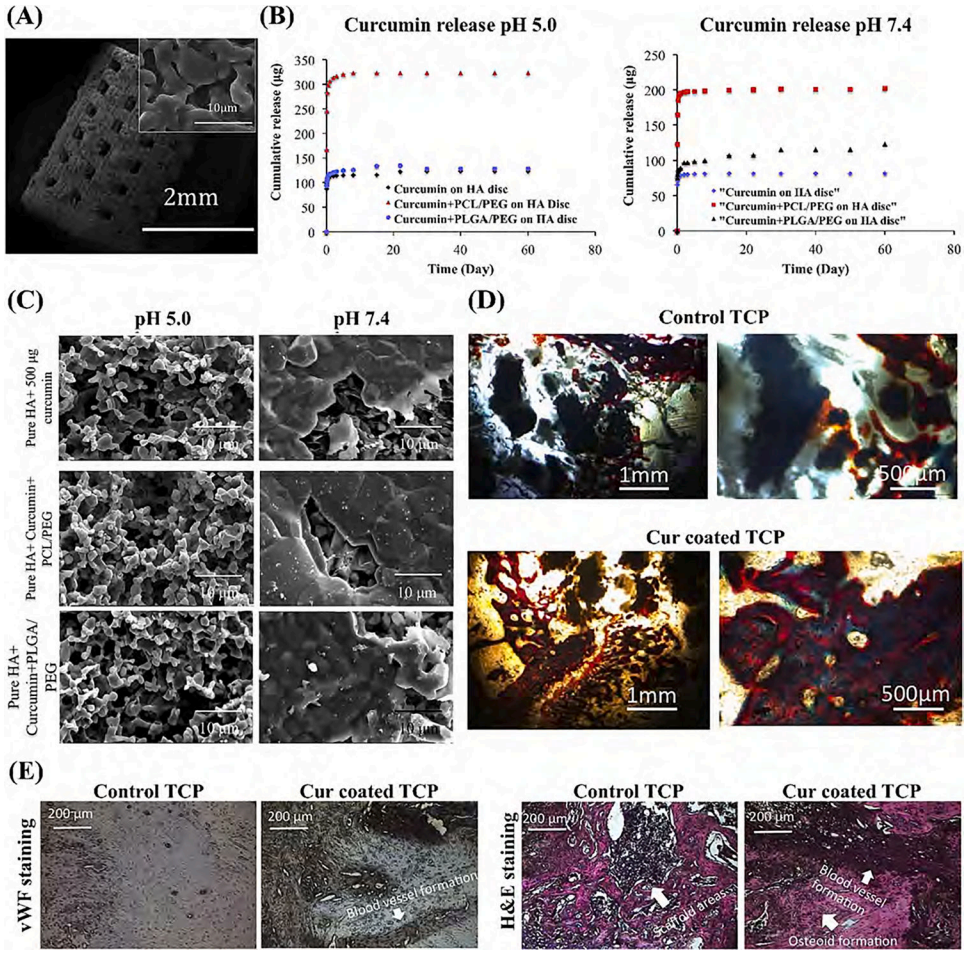


**Fig. 4.**

*In vivo* biological evaluation of controlled curcumin release from 3D printed ceramic scaffolds. (A) SEM images of curcumin-loaded scaffolds (Cur coated TCP). (B) Curcumin release from hydroxyapatite (HA) disc with and without polymer coating at pH 5.0 and pH 7.4. (C) SEM images of curcumin loaded HA with and without polymer coating at pH 5.0 and pH 7.4. (D) Modified Goldner's Masson trichrome staining images after 6 weeks (Reddish orange: osteoid, Green: mineralized bone). (E) vWF staining and H&E staining images after 6 weeks. Reproduced with permission [123]. Copyright 2018, Elsevier.
SEM, scanning electron microscopy; HA, hydroxyapatite; PCL, polycaprolactone; PEG, Polyethylene glycol; PLGA, poly(lactic-*co*-glycolic acid); TCP, tricalcium phosphate; Control TCP, 3D printed TCP scaffolds; Cur coated TCP, curcumin-loaded TCP scaffolds; vWF, von Willebrand factor; H&E, hematoxylin and eosin.

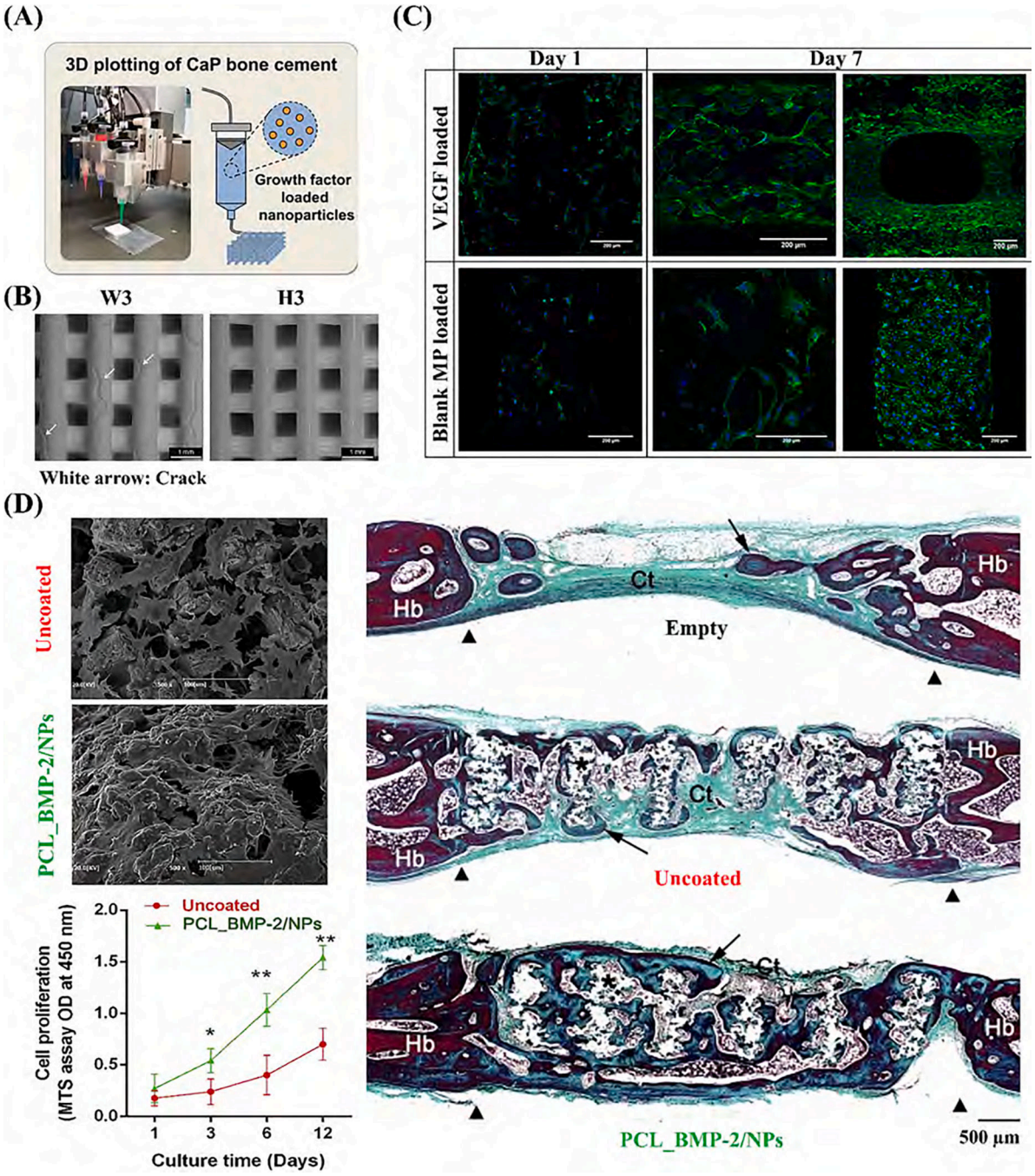


**Fig. 5.**

3D printed ceramic biomaterials as drug delivery vehicles. (A) Schematic image of the FDM manufactured calcium-phosphate-based scaffolds (CPC) incorporated with growth factor. (B) SEM images of CPC after immersion in water for 3 days (W3) and being held in a humid atmosphere for 3 days (H3) (White arrow: crack). (C) The confocal laser scanning microscopy images of human dermal microvascular endothelial cells (HDMEC) on day 1 and day 7 (shown with low and high magnification). Reproduced with permission [145]. Copyright 2015, Elsevier. (D) SEM images of human mesenchymal stem cell (hMSC)

proliferation on the scaffolds. (E) Mason Goldner's trichrome stained sections of the scaffolds. (The arrowhead: defect, The arrow: new bone, Hb: host bone, Ct: connective tissue). Reproduced with permission [146]. Copyright 2018, Elsevier.
CaP, calcium phosphate; CPC, calcium-phosphate-based scaffolds; SEM, scanning electron microscopy; W3, CPC after immersion in water for 3 days; H3, CPC after being held in a humid atmosphere for 3 days; VEGF, vascular endothelial growth factor; MP, microparticles, PCL; polycaprolactone; BMP-2, bone morphogenetic protein 2; NPs, nanoparticles; Hb, host bone; Ct, connective tissue; Uncoated, 3D printed HAp scaffold.

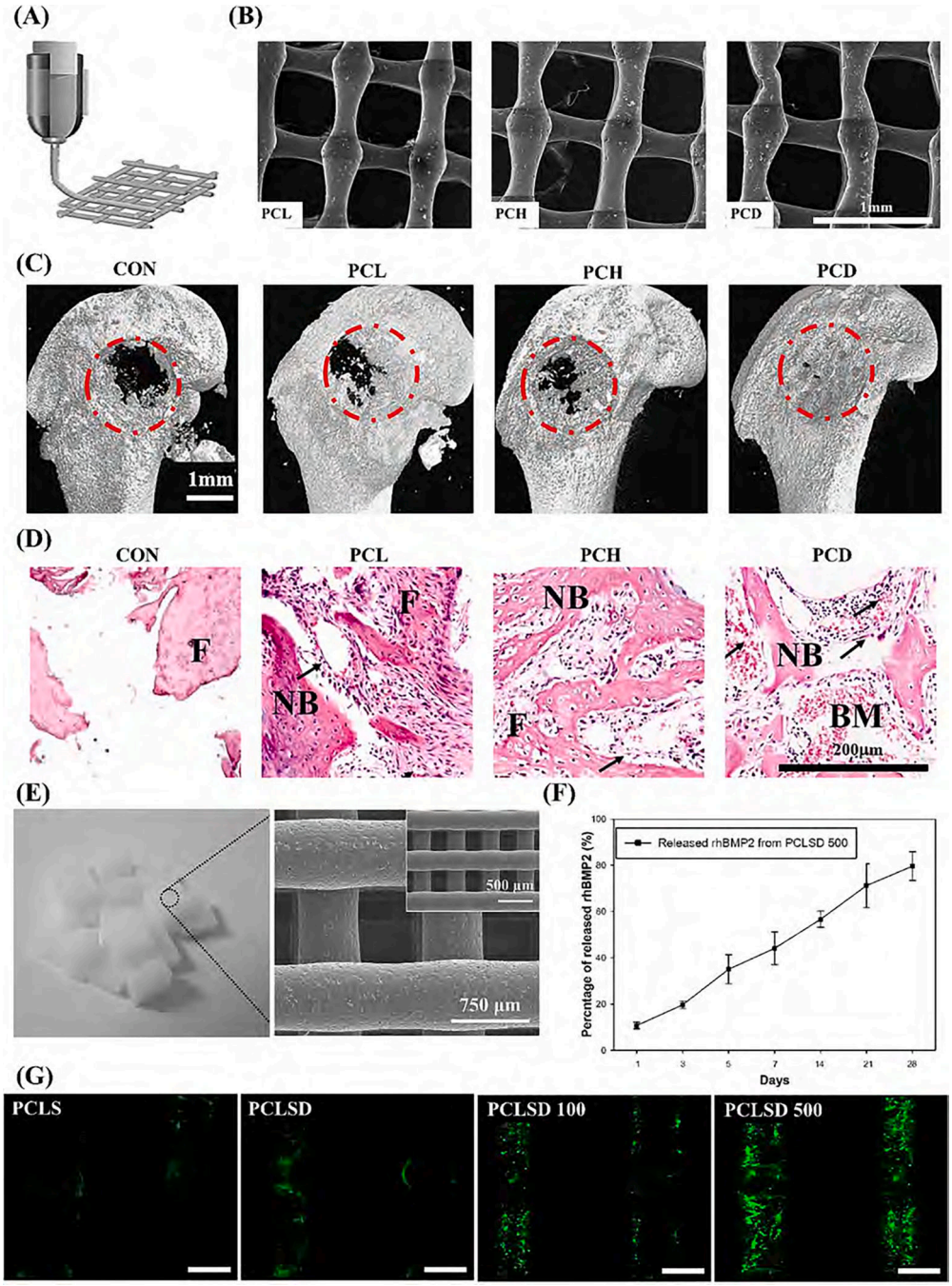


**Fig. 6.**

3D printed polymer biomaterials as drug delivery vehicles. (A) Fused deposition modeling (FDM) manufactured porous polycaprolactone (PCL) scaffolds. (B) SEM images of PCL scaffold, the intermediate aminated PCL scaffold (PCH) and carboxymethyl chitosan/deferoxamine loaded PCL scaffold (PCD). (C) Micro-CT examination of the effect of scaffolds on *in vivo* bone regeneration after 4 weeks. (D) Histological images after hematoxylin-eosin (HE) staining (The black arrow represents vascular formation, F: fibrous tissue, BM: newly formed bone marrow and NB: newly mineralized bone tissue). Adapted

from Ref. [156] with permission from Elsevier. Copyright (2018) Elsevier. (E) Digital images and SEM images of 3D printed PCL scaffold (PCLS). (F) The release profile of recombinant human bone morphogenic protein-2 (rhBMP2) loaded PCLS obtained in PBS (PCLSD 500). (G) The confocal laser scanning microscopy images of MC3T3-E1 cells on the scaffolds after 24 h. Adapted from Ref. [157] with permission from Elsevier. Copyright (2016) Elsevier.

FDM, fused deposition modeling; PCL, polycaprolactone; PCH, intermediate aminated PCL scaffold; PCD, carboxymethyl chitosan/deferoxamine loaded PCL scaffold; SEM, scanning electron microscopy; CON, rats without scaffolds; NB, newly mineralized bone tissue; F, fibrous tissue; BM, newly formed bone marrow; rHBMP, recombinant human bone morphogenic protein-2; PCLS, 3D printed PCL scaffold; PCLSD, dopamine coated PCL; PCLSD 100, PCLSD is immersed in rhBMP2 solution (100 ng/ml solution and 10 mM of Tris buffer) for 24 h; PCLSD 500, PCLSD is immersed in rhBMP2 solution (500 ng/ml solution and 10 mM of Tris buffer) for 24 h.

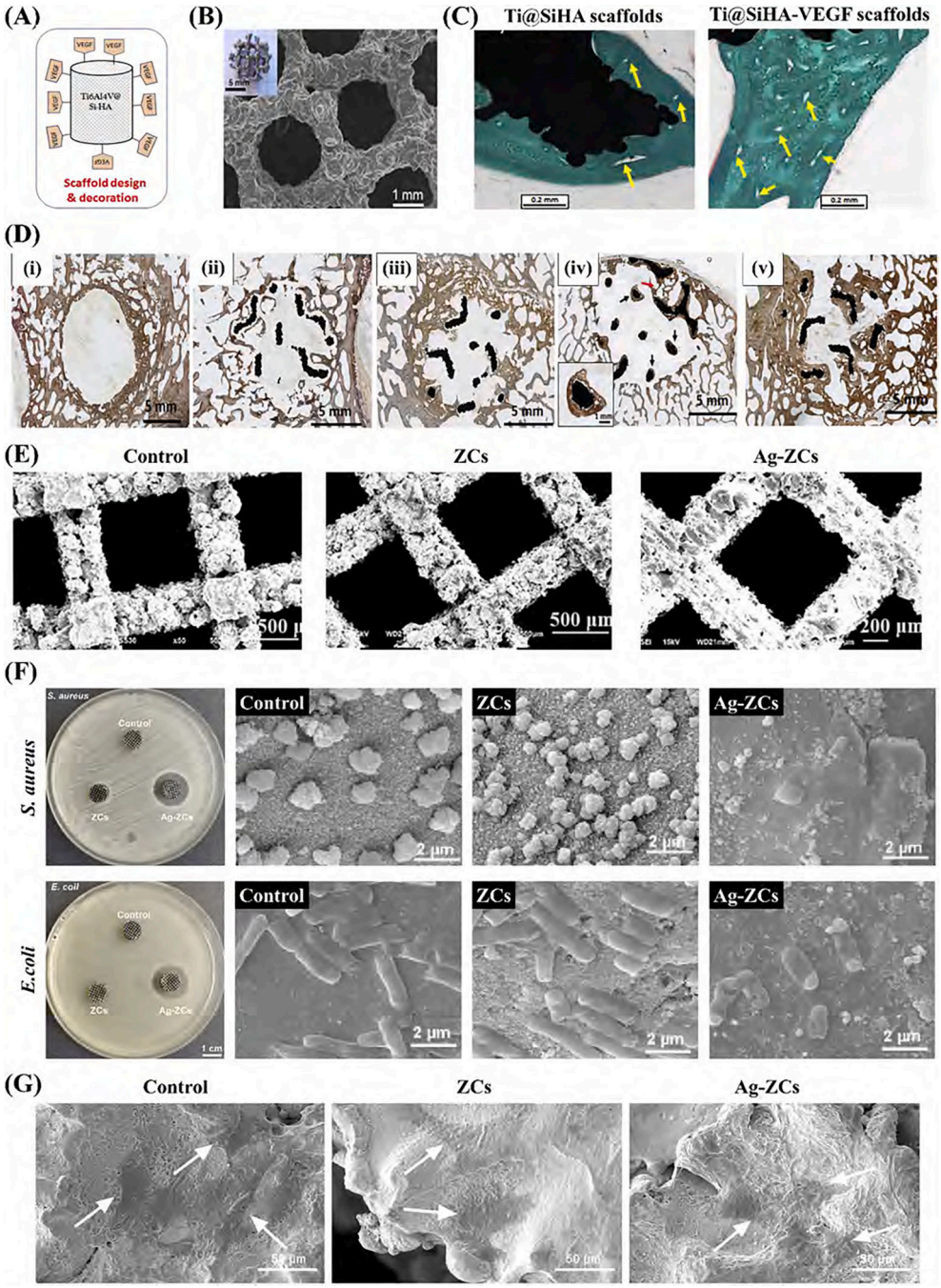


**Fig. 7.**

3D printed metal biomaterials as drug delivery vehicles. (A) Schematic image of vascular endothelial growth factor (VEGF)-incorporated SiHA-coated Ti6Al4V scaffolds. (B) The electron-beam melting (EBM) manufactured porous Ti6Al4V scaffold. (C) Optical microscopy images of histological sections after Masson-Goldner's trichrome staining (Yellow arrows: blood vessels). (D) Optical microscopy images of histological sections after von Kossa's staining. Reproduced with permission [172]. Copyright 2018, Elsevier. (E) SEM images of selective laser melting (SLA) manufactured porous 316 L stainless

steels: Control, ZCs, and Ag-ZCs. (F) Zone of inhibition assay to evaluate antibacterial properties toward *Staphylococcus aureus* and *Escherichia coli*. (G) SEM images of *in vitro* bone marrow stromal cells (BMSCs) at day 5. Reproduced with permission [173]. Copyright 2019, Elsevier.

SiHA, silicon substituted hydroxyapatite; VEGF, vascular endothelial growth factor; Ti@SiHA, silicon substituted hydroxyapatite coated Ti6Al4V scaffold; Ti@SiHA-VEGF, VEGF incorporated SiHA-coated Ti6Al4V scaffold; *S. aureus, Staphylococcus aureus*; *E. coli, Escherichia coli*; Control, selective laser melting manufactured porous 316 L stainless steels; ZCs, 316 L SS covered with a zeolite film; Ag-ZCs, Ag incorporated ZCs, SEM, scanning electron microscopy.

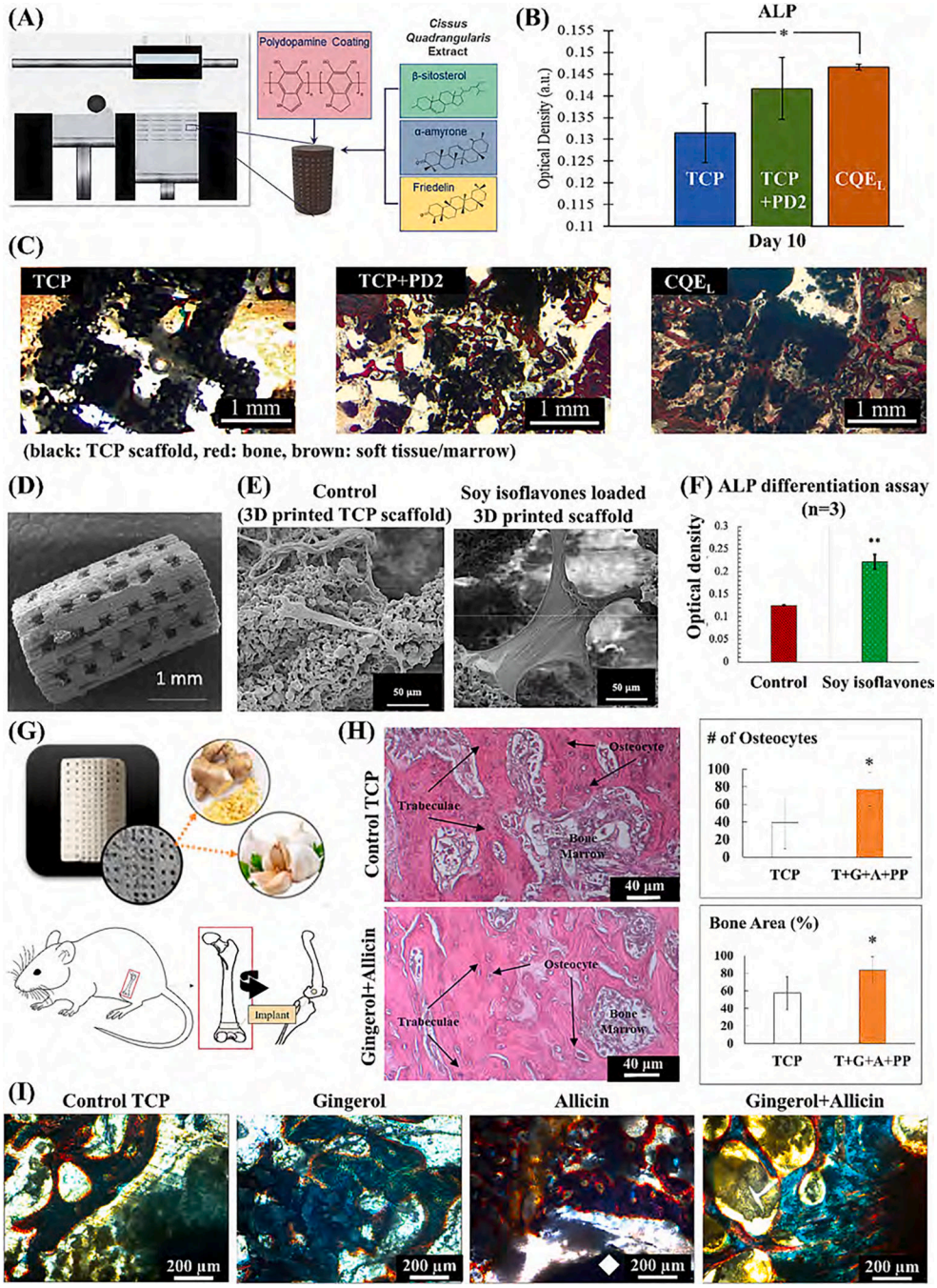


**Fig. 8.**

Drug delivery of NMCs from 3D printed scaffolds for bone regeneration. (A) Schematic representation of binder jetting printer and polydopamine coating with *cissus quadrangularis* extract (CQE) on 3D printed TCP. (B) ALP activity of osteoblast cells on scaffolds. (C) Masson Goldner staining images of the scaffolds. Reproduced with permission [121]. Copyright 2020, Elsevier. (D) SEM image of 3D printed TCP scaffold after sintering. (E) SEM images of *in vitro* osteoblast cells on the scaffolds in the bioreactor after 5 days. (F) Alkaline phosphatase (ALP) activity of osteoblast cells on the scaffolds. Adapted from Ref.

[18] with permission from Elsevier. Copyright (2020) Elsevier. (G) Schematic representation of *in vivo* study using gingerol and allicin loaded into a 3D printed TCP scaffold. (H) H&E staining images of 3D printed scaffolds at week 10. Histomorphometric analysis of osteocyte density and bone area from the scaffolds. (I) Optical micrographs of modified Masson-Goldner trichrome stained sections of the scaffolds at week 10 (Black: implant area). Reprinted with permission from Ref. [122]. Copyright 2022 American Chemical Society.

CQE, *cissus quadrangularis* extract; ALP, Alkaline phosphatase; TCP, tricalcium phosphate; TCP + PD2, polydopamine coated 3D printed TCP; CQEL, polydopamine coating with 200 μg of CQE; SEM, scanning electron microscopy; Control TCP, 3D printed TCP scaffold; Gingerol+Allicin, gingerol and allicin loaded 3D printed TCP scaffolds with polycaprolactone (PCL)/polyethylene glycol (PEG) coating; Gingerol, gingerol loaded 3D printed TCP scaffolds with PCL/PEG coating; Allicin, allicin loaded 3D printed TCP scaffolds with PCL/PEG coating.

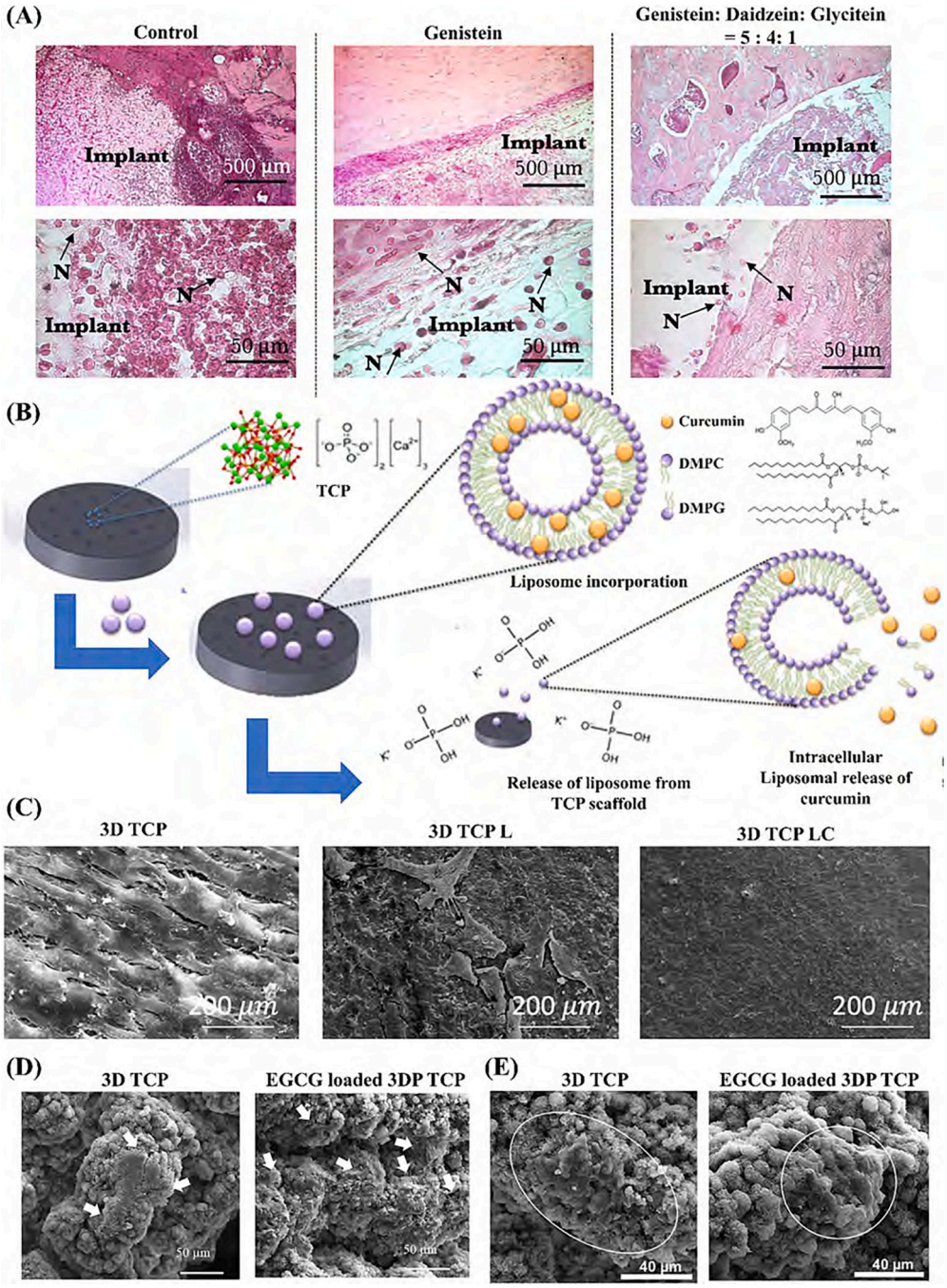


**Fig. 9.**

(A) Representative optical microscopy images of Hematoxylin and eosin (H&E) staining images after 24 h of implementation. Adapted from Ref. [18] with permission from Elsevier. Copyright (2020) Elsevier. (B) The chemical structure of liposome-encapsulated curcumin loaded on 3D printed TCP scaffold. (C) Scanning electron microscopy (SEM) images of *in vitro* osteosarcoma cells on 3D printed scaffolds. Reprinted with permission from Ref. [81] Copyright 2019 American Chemical Society. SEM images of *in vitro* (D) osteoblast cells

and (E) osteosarcoma cells on epigallocatechin gallate (EGCG) loaded 3D printed scaffolds. Reproduced from Ref. [191] with permission from the Royal Society of Chemistry. Control, 3D printed TCP scaffold; Genistein, genistein loaded 3D printed TCP scaffold;Genistein: Daidzein: Glycitein = (5:4:1): genistein, daidzein and glycitein mixed in 5:4:1 ratio to mimic their natural proportion found in soy and loaded on 3D printed TCP scaffold; DMPC, 1,2-dimyristoyl-sn-glycero-3-phosphocholine; DMPG, 1,2-Dimyristoyl-sn-glycero-3-phosphoglycerol; SEM, scanning electron microscopy; 3D TCP, 3D printed TCP scaffold; 3D TCP L, liposome-loaded 3D printed TCP; 3D TCP LC, liposomal curcumin loaded 3D printed TCP; EGCG, Epigallocatechin gallate.

**Table 1**

Role of various natural medicinal compounds (NMCs) in osteoporosis prevention.

| Natural medicinal compounds | Source | Major finding | Ref |
|---|---|---|---|
| Anabolic 3-ketosteroids | **Hadjod***(Cissus quadrangularis)* | • *C. quadrangularis* petroleum-ether extract promotes bone formation by decreasing bone loss and osteoclastic activity. ALP staining indicates that *C. quadrangularis* enhances new bone formation by enhancing osteoblast activity, while TRAP staining shows its anti-osteoclastic activity. | [24] |
| Rutin | **Buckwheat***(Fagopyrum esculentum)* | • Rutin has anti-osteoporotic activity. It improves bone mineral density in ovariectomized rats by enhancing the average bone volume percentage and thickness of trabecular bone. | [25] |
| Kaempferol | **Convolvulaceae***(Cuscuta chinensis)* | • Female rats administered with kaempferol show a substantial increase in bone volume fraction, Young's modulus, and trabecular bone perimeter but also a reduction in bone turnover. | [26] |
| Naringin | **Grapefruit** (*Citrus paradisi)* | • Mechanical strength of bone, bone volume, trabecular number, trabecular thickness, and bone mineral density in ovariectomized rats improved by a combination of naringin and treadmill exercise. | [27] |
| Resveratrol | **Grapes***(Vitis vinifera)* | • Ovariectomized rats fed a grape-enriched diet have improved bone quality, with increased net bone calcium retention, cortical thickness, and breaking strength. | [28] |
| Icariin | **Epimedium***(Epimedium brevicornum)* | • In the ovariectomized rat model, icariin-loaded calcium phosphate cement scaffolds promote angiogenesis and osteogenesis. Icariin enhances *in vitro* osteoblast differentiation by increasing OPG gene expression and inhibits *in vitro* osteoclast differentiation by decreasing RANKL gene expression. | [29] |
| Ginsenoside | **Ginseng***(Panax quinquefolius)* | • Ginsenoside-Rb2 enhanced the proliferation of MC3T3-E1 by preventing oxidative damage. It also increased calcium mineralization and alkaline phosphatase expression. The *in vivo* study showed that Ginsenoside-Rb2 enhanced bone mineral density. | [30] |

*C. quadrangularis, Cissus quadrangularis*; ALP, alkaline phosphatase; TRAP, Tartrate-resistant acid phosphatase; OPG, Osteoprotegerin; RNAKL, Receptor activator of nuclear factor kappa-B ligand.

**Table 2**

Role of various natural medicinal compounds (NMCs) in osteomyelitis prevention.

| Natural medicinal compounds | Source | Major finding | Ref |
|---|---|---|---|
| Allicin | **Garlic***(Allium sativum)* | • In an *in vivo* rabbit model, allicin inhibited growth of *Staphylococcus epidermidis*. Allicin also showed synergistic antibacterial activity against *Staphylococcus epidermidis* when combined with vancomycin. | [39] |
| Carvacrol | **Oregano** (*Origanum vulgare*) | • Oregano oil showed enhanced antimicrobial activity against MRSA, *Pseudomonas aeruginosa*, and *Acinetobacter baumannii* by effectively eradicating biofilms and damaging bacterial cells without any evidence of resistance development. | [40] |
| Curcumin | **Turmeric***(Curcuma longa)* | • Dual drug delivery of curcumin and erythromycin reduces bone infection, bacterial growth, and bacterial infection markers including TNF-α and IL-6. For MRSA-induced osteomyelitis in rats, the dual drug delivery system is more effective than either antibiotic alone. | [41] |
| Thymol | **Thyme***(Thymus vulgaris)* | • Thymol binds directly to the cell membrane of *Staphylococcus aureus*, thereby increasing membrane permeability and subsequently causes cell death. | [42] |
| Piperine | **Black Pepper***(Piper nigrum)* | • Piperine resulted in cell death of *Staphylococcus aureus by* increasing the permeability of antibiotics such as vancomycin and dicloxacillin. | [43] |
| Gingerol | **Ginger***(Zingiber officinale)* | • Molecular dynamic simulation analysis demonstrated that active compounds of ginger such as shogaol and gingernone-A have strong interactions with *Staphylococcus aureus* enzymes like enzyme HPPK, resulting in antibacterial activities. | [44] |
| Acemannan | **Aleo vera***(Aloe barbadensis miller)* | • *Aloe vera* extracts showed antibacterial properties toward *Staphylococcus aureus, Enterococcus faecalis*, *Escherichia coli* and *Pseudomonas aeruginosa*. It also inhibited *Escherichia coli* and *Enterococcus faecalis* biofilm. | [45] |

MRSA, methicillin-resistant *Staphylococcus aureus*; TNF-α, tumor necrosis factor alpha; IL-6, interleukin 6; HPPK, 6-hydroxymethyl-7,8-dihydropterin pyrophosphokinase.

**Table 3**

Role of various NMCs in osteosarcoma prevention.

| Natural medicinal compounds | Source | Major finding | Ref |
|---|---|---|---|
| Curcumin | **Turmeric** (*Curcuma longa*) | • Curcumin doses ranging from 5 μM to 25 μM show higher cytotoxicity toward MG-63 osteosarcoma cells, but osteoblast cells survived with higher than 80% viability after 24 h. Curcumin has the potential to selectively kill bone cancer cells without damaging healthy bone cells if combined with a suitable drug delivery vehicle. | [57] |
| Epigallocatechin gallate (EGCG) | **Green Tea** (*Camellia sinensis*) | • EGCG limits the ability of osteosarcoma cells to migrate and invade *via* decreasing the mitogen-activated protein kinase kinase/extracellular signal-regulated kinase signaling pathway. | [58] |
| Artemisinin | **Sweet wormwood plant,** (*Artemisia annua*) | • The mouse *in vivo* osteosarcoma model shows that artemisinin reduces osteosarcoma growth by decreasing angiogenesis *via* the p38 MAPK/CREB/TSP1 signaling pathway. | [59] |
| Berberine | **Berberis** (*Berberis vulgaris*) | • Berberine inhibits the PI3K/Akt signaling pathway, which prevents the proliferation of U2OS osteosarcoma cells and induces apoptosis of the cells. | [60] |
| Ginsenoside | **Ginseng** (*Panax ginseng*) | • Ginsenoside inhibits cell growth and induces apoptosis in human osteosarcoma cells (MG-63 and SaOS2) by increasing the expression of cleaved caspase-3 and Bax and decreasing the expression of cyclin D1, Bcl-2 and β-catenin. | [61] |
| Wogonin | **Baikal skullcap** (*Scutellaria baicalensis*) | • Wogonin induces the apoptosis of U2OS osteosarcoma cells through caspase 3 pathways, mitochondrial dysfunction, and endoplasmic reticulum stress. | [62] |
| Emodin | **Rhubarb** (*Rheum rhabarbarum* | • Emodin promotes apoptosis of U2OS osteosarcoma cells by causing mitochondrial dysfunction and endoplasmic reticulum stress. | [63] |
| Silibinin | **Milk thistle** (*Silybum marianum*) | • Silibinin prevents osteosarcoma MG-63 cell attachment by aggregating microfilaments and changing the shape of the cell to round and shrunken. Silibinin also inhibits the ability of MG-63 osteosarcoma cells to invade by suppressing matrix metalloproteinase-2 and the urokinase-type plasminogen activator. | [64] |
| Punicalagin | **Pomegranate***(Punica granatum)* | • Punicalagin inhibits the NF-κB signaling pathway, causing cytotoxicity in human osteosarcoma cell lines (MG-63, U2OS, and SaOS2). It also inhibits the growth of U2OS and SaOS2 tumors in mouse models. Punicalagin has no cytotoxicity to human osteoblast cells (hFOB1.19) at concentrations less than 100 μM. | [65] |

EGCG, epigallocatechin gallate; MAPK, mitogen-activated protein kinase; CREB, cAMP response element-binding protein; TSP1, thrombospondin-1; PI3K, Phosphoinositide 3-kinase; Akt, protein kinase B; BAX, Bcl-2-associated X protein; Bcl-2, B-cell lymphoma 2.

**Table 4**

Role of various NMCs in osteoarthritis prevention.

| Natural medicinal compounds | Source | Major finding | Ref |
|---|---|---|---|
| Capsaicin | **Chili Peppers***(Capsicum annuum)* | • In licensed doses, topical non-steroidal anti-inflammatory drugs and capsaicin are equally helpful for pain management in OA. | [74] |
| Gingerol | **Ginger***(Zingiber officinale)* | • Study showed a statistically significant reduction in knee OA symptoms in 247 patients after taking ginger extract. | [75] |
| Salicin | **Willow bark***(Salix alba)* | • Salicin inhibits the NF-κB proinflammatory signaling pathway and prevents the degradation of type II collagen and aggrecan, all while minimizing oxidative stress. It has potential to be a safe and effective treatment of OA. | [76] |
| Curcumin | **Turmeric***(Curcuma longa)* | • Curcumin is more tolerable than diclofenac in patients with knee OA. Patients with knee OA who are unable to tolerate the negative effects of non-steroidal anti-inflammatory medicines can benefit from using curcumin as an alternate therapy option. | [77] |
| Terpenoids | **Gingko***(Ginkgo biloba)* | • Gingko suppresses JNK activation and promotes c-Jun degradation, which protect chondrocytes against degeneration. Gingko can be used as a therapeutic agent to treat OA. | [78] |
| Quercetin | **Onion***(Allium cepa)* | • Quercetin alleviates OA symptoms in an OA rat model by inhibiting IL-1β and TNF-α production *via* the TLR-4/NF-κB pathway. | [79] |

OA, osteoarthritis; NF-κB, nuclear factor kappa B; JNK, c-Jun N-terminal kinas; IL-1β, interleukin-1 beta; TNF-α, Tumor necrosis factor alpha; TLR-4, toll-Like Receptor 4.

**Table 5**

Various 3D printed bone substitutes for local delivery of therapeutic molecules used in different bone-related complications.

| Material | | AM Process | Coating material | Therapeutic loaded | Strategy of the controlled release | Major findings for bone health | Ref |
|---|---|---|---|---|---|---|---|
| Metal | Ti6Al4V | EBM | SiHA | VEGF | The presence of a SiHA coating on these structures accelerates the adsorption of VEGF. | VEGF-loaded scaffolds enhance the proliferation of MC3T3-E1 osteoblast cells and endothelial cells *in vitro*. The scaffolds also increase new bone formation in an osteoporotic sheep. | [172] |
| | 316 L stainless steel | SLM | Zeolite | AgNO3 | Zeolite coating controlled release rate of $AgNO_3$. | The release of $Ag^+$ prevents the adhesion and growth of bacteria such as *Escherichia coli* and *Staphylococcus aureus*. It also promotes osteogenic differentiation of BMSCs. | [173] |
| | Ti6Al4V | SLM | PLGA | 2,5-Dihydroxybenzoic acid | The PLGA coating induces a burst release of 2,5-Dihydroxybenzoic acid within the first 7 days, followed by a sustained release. | E-2,5-DHB release from PLGA- coated scaffolds increase new bone formation as well as inhibit bone resorption in osteoporotic model rats. | [180] |
| | Ti6Al4V | EBM | Polydopamine | Nano silver encapsulated silk fibrin | Ag + showed an early burst release followed by sustained release for 42 days. | The released nanosilver from silk fibrin incorporated with Ti6Al4V scaffolds stimulates proliferation and osteoblastic differentiation of MC3T3-E1 cells as well as shows antibacterial properties for planktonic and *Staphylococcus aureus* bacterial cells. | [181] |
| | Ti6Al4V | EBM | PVA | Vancomycin hydrochloride | Vancomycin hydrochloride was released from PVA coating | The release of vancomycin hydrochloride promotes bone regeneration and antimicrobial activity in rats infected with *Staphylococcus aureus*. | [182] |
| Polymer | PCL | FDM | Alginate | BMP-2/UCS | BMP-2/UCS showed simultaneous release with low dosage due to alginate coating | The BMP-2 and UCS loaded scaffolds enhance *in vitro* and *in vivo* osteogenesis. | [183] |
| | PCL | FDM | Chitosan | Deferoxamine | Deferoxamine with chitosan coating showed an initial fast release followed by slow release. | The release of deferoxamine from scaffolds improves angiogenesis and osteogenesis both *in vitro* and *in vivo*. | [156] |
| | PCL | FDM | – | Alendronate | The release of alendronate was found to be faster at pH 5.0 compared to pH 7.4 due to the faster degradation of PCL in acidic solutions. | The alendronate-loaded PCL scaffolds enhance the osteoblast activity and mineralization of MG-63 cells compared to a PCL-only scaffold. In a rat tibial defect model, the drug-loaded scaffolds promote bone formation compared to the control. | [184] |
| | PCL/PEG | FDM | – | ROX | The increased hydrophilicity of scaffolds with PEG coating resulted in increased ROX release. | The ROX-incorporated composite scaffold has antibacterial effects against *E. coli* and *S. aureus*. The drug loaded scaffold shows good viability and growth of human osteoblast-like cells. | [185] |
| | PCL | FDM | Polydopamine | BMP-2 | For 28 days, BMP-2 showed a sustained release rate with polydopamine coating. | The BMP-loaded scaffold improves cell proliferation and osteoconductivity of osteoblastic MC3T3-E1 cells in comparison with control. | [157] |
| | PCL | FDM | Chitosan/TCP/ Clay | DOX | DOX release from the scaffold prolongs. | The DOX-loaded scaffolds inhibit the viability of human osteosarcoma MG-63 cells compared to control. | [186] |

| Material | | AM Process | Coating material | Therapeutic loaded | Strategy of the controlled release | Major findings for bone health | Ref |
|---|---|---|---|---|---|---|---|
| | PCL | FDM | Collagen | PLGA encapsulated simvastatin | Simvastatin encapsulated in PLGA showed sustained release for over 27 days. | *In vitro* studies show that the simvastatin-loaded scaffold improves cell viability and the osteogenic differentiation of BMSCs compared with the control. Simvastatin release from the scaffold improves *in vivo* new bone regeneration compared to control. | [187] |
| | CFC | FDM | – | Chitosan encapsulated VEGF | VEGF showed an initial burst release followed by a sustained release. | The VEGF-loaded scaffolds show enhanced cell attachment and the proliferation of HDMEC compared to control scaffolds. | [145] |
| | HA | FDM | Collagen | rhBMP-2 | rhBMP-2 showed initial burst release followed by a sustained release. | The rhBMP-2-loaded scaffolds promote *in vitro* osteogenic differentiation of human mesenchymal stem cells and enhance *in vivo* bone regeneration. | [188] |
| Ceramic | | | | | | | |
| | HA | Binder jetting | PCL | BMP-2 loaded nanoparticles | After an initial slow release over the first 3 days, BMP-2 with PCL coating showed sustained release. | BMP-2-loaded nanoparticles-coated scaffold enhances adhesion, proliferation and osteogenic differentiation of human mesenchymal stem cells compared to control. It also shows more *in vivo* bone regeneration than the control group. | [146] |
| | HA/TCP | FDM | Collagen | Dipyridamole or BMP-2 | When coated with collagen, dipyridamole showed sustained release. | In the histological analysis, both dipyridamole-loaded scaffolds and BMP-2-loaded scaffolds increased bone formation. | [189] |
| | TCP | FDM | Polydopamine | Melatonin | In the presence of the polydopamine coating, melatonin exhibited a slower release rate | Melatonin release from a dopamine- coated scaffold enhances the viability and proliferation of mouse bone mesenchymal stem cells. The scaffold also increases osteogenesis-related genes *in vitro* and new bone formation in a rat model *in vivo*. | [144] |
| | BCP | Binder jetting | – | BMP-2 | NA | *In vivo* study shows that the BMP-2-loaded scaffold has enhanced the osteogenic capacity compared to the control group. | [190] |
| | TCP | Binder jetting | PCL/PEG | Allicin | Allicin was loaded with a polymer mixture of 65:35 M ratio of PCL and PEG to control the release of allicin. | Allicin-loaded 3D printed tricalcium phosphate scaffolds enhance angiogenesis and osteogenesis. | [122] |
| | TCP | Binder jetting | PCL/PEG | Gingerol | Gingerol was loaded with a polymer mixture of 65:35 M ratio of PCL and PEG to control release of gingerol. | Gingerol-loaded 3D printed tricalcium phosphate scaffolds promote bone formation and blood vessel growth. | [122] |
| | TCP | Binder jetting | | Soy isoflavones | Controlled release of soy isoflavones was achieved by (1) hydrophobic interaction and competitive electrostatic interaction between soy isoflavones, (2) scaffold degradation, (3) drug solubility change, and (4) drug-protein complex formation. | Soy isoflavones-loaded 3D printed TCP scaffolds improve proliferation and differentiation of human fetal osteoblastic cells compared to control TCP scaffold. | [18] |
| | TCP | Binder jetting | DMPC-DMPG | Curcumin | Liposome-encapsulated curcumin showed more sustained release than free curcumin. | Liposomal curcumin inhibits osteosarcoma cell growth and viability *in vitro* by 96% compared to control 3D printed bone scaffold without curcumin. | [81] |
| | TCP | Binder jetting | – | Epigallocatechin Gallate | Deprotonated EGCG at physiological pH showed higher release at pH 7.4. | EGCG -loaded 3D printed TCP scaffolds enhance *in vitro* osteoblast cell proliferation by upregulating Runx2 | [191] |

| Material | | AM Process | Coating material | Therapeutic loaded | Strategy of the controlled release | Major findings for bone health | Ref |
|---|---|---|---|---|---|---|---|
| | | | | | | and BGLAP expression. EGCG release inhibits *in vitro* osteosarcoma proliferation. | |
| | HA/PCL | FDM | PLGA-PEG-PLGA hydrogel | BMP/VEGF | Both BMP-2 and VEGF-165 exhibited an initial burst release, followed by sustained release over a period of 21 days | The synergistic effect of BMP- and VEGF-loaded scaffolds improves *in vitro* osteogenic differentiation of MC3TC and *in vivo* ectopic ossification. | [192] |
| Composite | SiO2/PCL | FDM | – | Ruthenium loaded PEGylated liposomes | Internal pore structure of the scaffolds impeded the release of PEGylated liposomes containing ruthenium resulting in a slow release rate. | The Ruthenium-loaded PEGylated liposome scaffold reduces MG-63 osteosarcoma cell viability after 24 h and triggers mitochondrial dysfunction of the cell apoptosis. | [193] |

PCL, polycaprolactone; CFC BCP, biphasic calcium phosphate; HA, hydroxyapatite; EBM, electron beam melting; SLM, selective laser melting; FDM, fused deposition modeling; PLGA, Polylactic-co-glycolic acid; PVA, Polyvinyl alcohol; TCP, Tricalcium phosphate; rhBMP-2, recombinant human bone morphogenetic protein-2; PEG, Polyethylene glycol; BMP-2, Bone morphogenetic protein-2; UCS; umbilical cord serum, ROX, roxithromycin; PEG, polyethylene glycol; Runx2, Runt-related transcription factor 2; BGLAP, bone gamma-carboxyglutamic acid-containing protein; DMPC, 1,2-dimyristoyl-sn-glycero-3-phosphocholine; DMPG, 1,2-dimyristoyl-sn- glycero-3-phospho-(1′-rac-glycerol).